JOURNAL OF PETROLOGY | VOLUME 44 | NUMBER 9 | PAGES 1619–1656 | 2003 | DOI: 10.1093/petrology/egg051

The Origin of Basic–Ultrabasic Sills with S-, D-, and I-shaped Compositional Profiles by *in Situ* Crystallization of a Single Input of Phenocryst-poor Parental Magma

RAIS M. LATYPOV*

GEOLOGICAL INSTITUTE, KOLA SCIENCE CENTRE, APATITY, 184200, RUSSIA

RECEIVED FEBRUARY 8, 2002; ACCEPTED MARCH 7, 2003

An attempt is made to develop an in situ *crystallization model based on the concept of Soret fractionation to explain the origin of commonly observed S-, D-, and I-shaped compositional profiles in sills formed from a single pulse of phenocryst-poor parental magma. The model envisages that the various compositional profiles observed in sills can be interpreted in terms of different combinations of four principal units—Basal Zone and Layered Series forming the floor sequence, and Top Zone and Upper Border Series constituting the roof sequence. The Basal and Top Zones represent mirror images of the Layered and Upper Border Series, respectively, and therefore are referred to as basal and top reversals. It is proposed that the formation of basal and top reversals takes place through the non-equilibrium Soret differentiation of liquid boundary layers which form as a consequence of the temperature gradient imposed by the cold country rock. In contrast, the Layered and Upper Border Series originate predominantly through the crystal–liquid boundary layers developing in equilibrium conditions. The model permits the production of S-, D-, and I-shaped compositional profiles from the same magma composition. All that is necessary to produce a specific shape of compositional profile is an appropriate temperature gradient imposed by the cold country rock on the liquid boundary layers of a parental magma of a given composition.*

KEY WORDS: *sills; compositional profiles;* in situ *crystallization; Soret fractionation*

INTRODUCTION

The study of basic–ultrabasic sills may provide some of the best insights into the processes leading to the differentiation of natural silicate magmas. Sills usually show complete rock sequences including roof and basal chilled zones, which provide information about phase, modal and cryptic layering of magmatic bodies. Apart from those examples where multiple intrusions are involved, the bulk composition of sills can provide a reliable estimate of the parental magma composition, which is of paramount importance for any model of magma differentiation. The course of emplacement and solidification is also commonly clear in sills, allowing resolution of the conflict over whether the final rock sequence was produced by a single injection or by multiple injections.

Three main types of basic–ultrabasic sill have been identified on the basis of the shape of the modal mineralogical variation, or MgO and SiO_2 compositional profile as a function of stratigraphic height (Gibb & Henderson, 1992; Marsh, 1996); these are sills with S-, D- and I-shaped compositional profiles (Fig. 1). The well-known S-type sills are the most differentiated bodies, which are characterized by high concentrations of olivine near the base (Gray & Crain, 1969; Fujii, 1974; Frenkel' *et al.*, 1988, 1989; Marsh, 1989). The term D-type sill was introduced to distinguish bodies in which modal olivine contents tend to decrease towards

*Corresponding author. Present address: Institute of Geosciences, P.O. Box 3000, FIN—90014, University of Oulu, Oulu, Finland. Telephone: +358 8 553 1452. Fax: +358 8 553 1484. E-mail: rais.latypov@oulu.fi

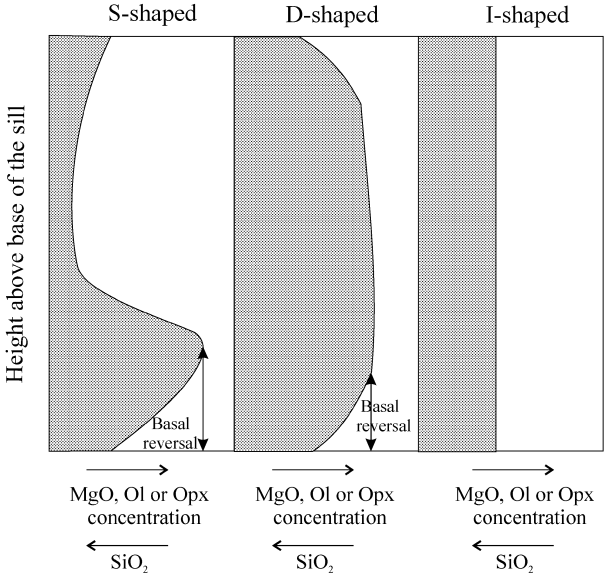

Fig. 1. Schematic vertical compositional profiles of components (e.g. MgO and SiO_2) or modal abundance of olivine and orthopyroxene in S-, D-, and I-shaped sills. The well-developed basal reversals in the S- and D-shaped sills should be noted. (See text for further explanation.)

the upper and lower margins in a roughly symmetrical manner (Gibb & Henderson, 1992). The name I-type sill (Marsh, 1996) is used for bodies showing little field, petrographic or geochemical evidence of differentiation and displaying neither well-developed cumulate zones nor late-stage differentiates (Gunn, 1966; Froelich & Gottfried, 1988; Mangan & Marsh, 1992).

There have been several attempts to resolve the problem of the existence of sills with S-, D- and I-shaped compositional profiles (see discussion by Simkin, 1967; Gibb & Henderson, 1992; Marsh, 1996). Different mechanisms have been suggested to explain this phenomenon. Among them are a gravity-induced settling of crystals, either already present in the magma at the time of emplacement (Gray & Crain, 1969; Fujii, 1974; Marsh, 1989) or newly grown in the magma chamber (Frenkel' *et al*., 1988, 1989; Woster *et al*., 1990, 1993), flow differentiation (Komar, 1972; Marsh, 1996), multiple injection of distinct magmas with different compositions (Gibb & Henderson, 1992; Czamanske *et al*., 1994, 1995), and the convective flux of refractory components within the crystal–liquid mush of the boundary layer during *in situ* differentiation (Tait & Jaupart, 1996). All of the above processes are probable and, in some circumstances, can contribute to the final shape of the compositional profiles. They are unlikely, however, to represent the dominant explanation for the appearance of sills with different compositional profiles because they are unable to explain the formation of the basal and top reversals that represent the distinctive characteristic feature of many sills (Latypov, 2003).

In this paper a model is developed that can explain the origin of all types of compositional profiles in sills formed from a single pulse of phenocryst-poor or phenocryst-free parental magma. By a single pulse I imply here that the sills are filled to their present width continuously with the same magma composition on a time scale much shorter than that of solidification. The model represents a combination of the model of *in situ* crystallization in thermal boundary layers of Tait & Jaupart (1996) with a mechanism for the origin of marginal reversals by Soret fractionation (Latypov, 2003).

REVIEW OF SILLS WITH DIFFERENT COMPOSITIONAL PROFILES AND CURRENT MODELS FOR THEIR FORMATION

Description of sills with S-, D- and I-shaped compositional profiles

In the following discussion I shall adhere to the conventional classification of sills into those with S-, D- and I-shaped profiles (Fig. 1) although I find that this division is rather schematic and does not embrace all the types of compositional profiles that are observed in nature.

S-shaped profiles

The best descriptions of the typical S-shaped sills are provided by detailed studies of differentiated alkaline sills of Skye, Scotland (Drever & Johnston, 1967; Simkin, 1967), picrite–gabbro–dolerite sills of the Noril'sk region, Russia (Distler *et al*., 1979; Czamanske *et al*., 1994, 1995; Turovtsev *et al*., 2000), and dolerite sills of Antarctica (Gunn, 1966). Modal variations in vertical sections through most alkaline S-shaped sills (Fig. 2a–c) typically show an olivine-poor lower zone followed by a rapid, but gradational, increase in the amount of olivine to a picrite unit that constitutes one-half to three-quarters of the sill thickness. The picrite unit with 30–50 vol. % olivine is succeeded abruptly by an olivine-poor picrodolerite–analcime gabbro unit with ~10 vol. % Ol, which continues to the upper margin. Such discontinuities between rocks relatively rich and poor in olivine are observed in nearly all alkaline dolerite sills and are commonly rather sharp (Simkin, 1967). Gibb & Henderson (1989) and Gibson & Jones (1991) reported that the sharp breaks are also marked by interior chills, whereas Simkin (1967, p. 64), in contrast, argued that there is no evidence for interior chilling at these discontinuities.

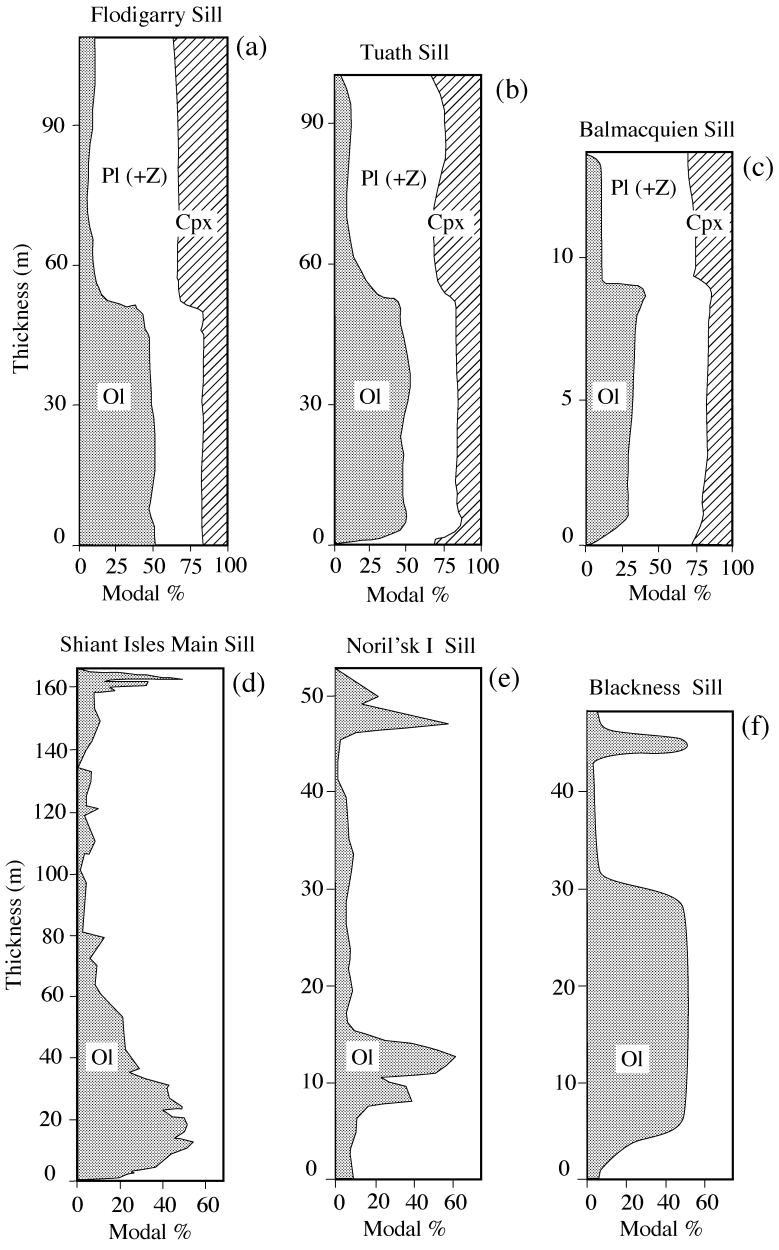

Fig. 2. S-shaped (a–c) and double-humped (d–f) modal profiles in selected sills. The S-shaped sills are characterized by olivine-poor zones in the upper parts and olivine-rich zones in the lower parts of the sills. The double-humped sills are a variety of the S-shaped sills with thin upper olivine-rich units. Based on the following data sources: a–c, Simkin (1967); d, Foland *et al.* (2000); e, Turovtsev *et al.* (2000); f, Flett (1931). In (d)–(f) only variations in olivine content are shown. It is unclear from Simkin (1967) whether the basal reversal in Ol content is absent from the Flodigarry sill (a) or is not observed because of poor exposure. Hereafter in figures and text: Pl, plagioclase; Ol, olivine; Opx, orthopyroxene; Pig, pigeonite; Cpx, clinopyroxene; Qtz, quartz; Z, zeolite.

Similar modal variations are observed in most sills in the Noril'sk region, where a relatively sharp, unchilled contact between picritic gabbro–dolerite and overlying olivine gabbro–dolerite is marked by an abrupt decrease in olivine content from 50–60 vol. % to 10–20 vol. %. Passing upwards from olivine gabbro–dolerite to olivine-bearing gabbro–dolerite, and then to prismatic and magnetite gabbro, the amount of olivine decreases further until it completely disappears. The transition from picritic units to underlying taxitic gabbrodolerite in these sills is characteristically gradational. An important peculiarity of many

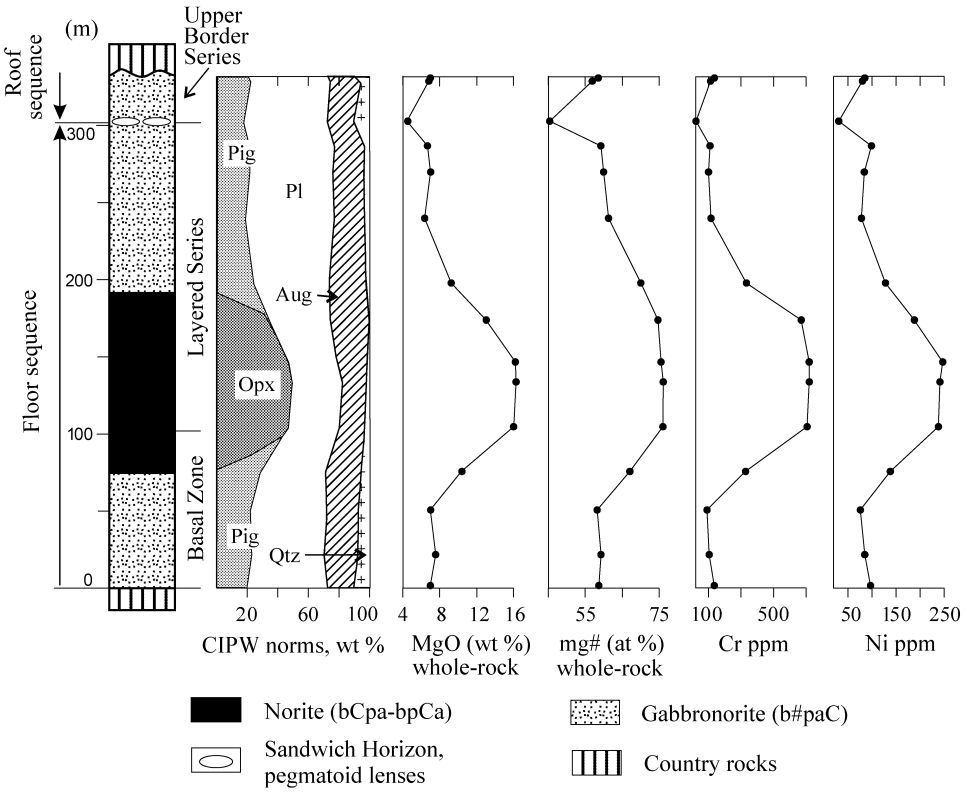

Fig. 3. Generalized stratigraphic section through the Lake Vanda sill (Antarctica) showing a profile intermediate between S- and D-shaped in CIPW normative mineralogy and in whole-rock MgO, mg-number, Cr and Ni contents. Data from Gunn (1966). mg-number = 100Mg/($Mg + Fe^{2+} + Fe^{3+}$). Hereafter in abbreviations of cumulates: o, olivine; p, plagioclase; a, clinopyroxene; b, orthopyroxene; b#, pigeonite and inverted pigeonite; C, cumulate. Symbols preceding C denote cumulus phases; those following C denote intercumulus phases.

Siberian picrite–gabbrodolerite sills (Lebedev, 1957; Zolotuhin & Vasil'ev, 1967; Ivanov *et al.*, 1971; Ryabov, 1992; Turovtsev *et al.*, 2000) and some alkaline sills (Drever & Johnston, 1967; Gibb & Henderson, 1996; Foland *et al.*, 2000) is the occurrence of upper olivine-rich units (Fig. 2d–f). It is noteworthy that the modal and mineral compositions of such units cover practically the whole range of rock compositions from the entire intrusion section (Duzhikov & Distler, 1992; Gibb & Henderson, 1996). This type of compositional variation, which I refer to as a 'double-humped' profile, is classified here as a variety of the S-shaped profile.

Typical S-shaped compositional profiles are also exhibited by Antarctic dolerite sills (Gunn, 1962, 1966). These sills usually include a thick layer of hypersthene gabbro or norite centred somewhat below the middle of the sills and commonly making up a third of the entire bulk of the sill. This lithology grades abruptly or gradationally both above and below into a pigeonitic dolerite in which orthopyroxene is entirely absent. This transition is accompanied by a marked decrease in whole-rock mg-number, and Cr and Ni concentrations. A generalized stratigraphic section through one such sill, at Lake Vanda, showing a profile intermediate between S- and D-shape, is shown in Fig. 3.

D-shaped profiles

Some typical examples of D-shaped sills, which are distinguished by thick olivine-rich central units, and roughly symmetrical olivine-poor upper and lower margins, are illustrated in Fig. 4. The most primitive bulk compositions in such sills are not at the margins but near the middle; the most evolved compositions are at the chilled margins (Marsh, 1996). Compositional profiles through the D-type Lugar sill, Scotland, are shown in Fig. 5. Here, the central olivine-rich unit consists mainly of picrite and minor kaersutite nepheline gabbro and nepheline gabbro. It is noteworthy that the four uppermost analcime gabbro units are mirror images of the four bottom units, both being the most evolved rocks in the sill in terms of major and trace elements.

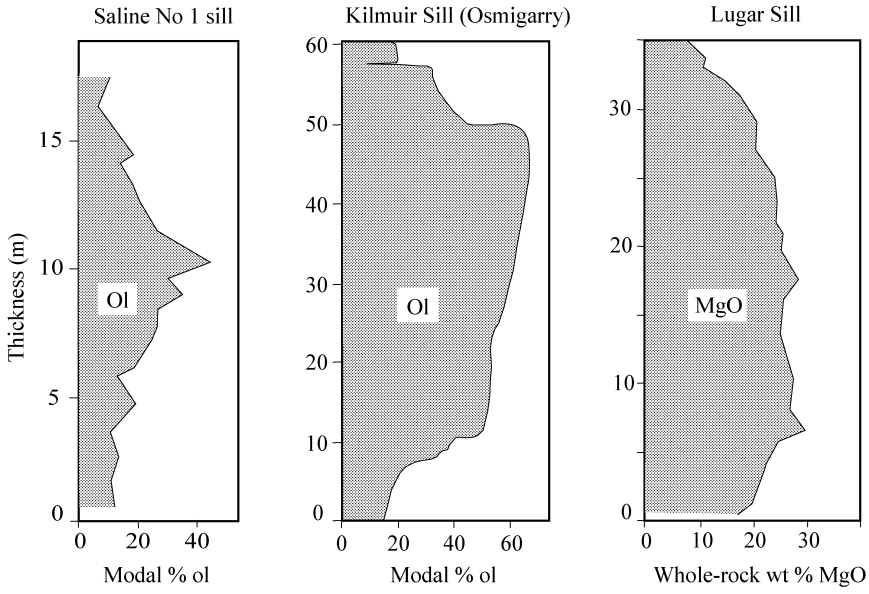

Fig. 4. D-shaped modal profiles in selected sills. The D-shaped sills are distinguished by modal olivine or whole-rock MgO contents tending to decrease in a roughly symmetrical manner towards the upper and lower margins. Data from Gibb & Henderson (1992).

I-shaped profiles

The existence of I-shaped profiles through sills and lava flows, which exhibit very little modal or whole-rock chemical variation, has been noted by many petrologists (Gunn, 1966; Froelich & Gottfried, 1988; Mangan & Marsh, 1992). It is repeatedly stressed that the bodies displaying I-shaped profiles are remarkably undifferentiated, show no cumulates and have no systematic vertical chemical zonation despite being sometimes up to 400–500 m thick (Fig. 6). It should, however, be noted that many sills of interest are I-shaped only in terms of modal composition or major elements such as SiO_2 and MgO. In terms of mg-number and trace elements, they can reveal fairly well-developed compositional profiles. As an example, the New Mountain sill, Antarctica, despite having an I-shaped modal profile, exhibits a typical S-shaped cryptic profile in terms of mg-number, Cr and Ni (Fig. 7). It is therefore incorrect to consider that these types of sills do not exhibit evidence of differentiation. Most of them, if not all, show evidence of fairly well-developed differentiation, especially in terms of trace elements, which are the most sensitive indicators of magma evolution for this type of sill.

Current models for the formation of S-, D- and I-shaped compositional profiles in sills

Four principal mechanisms have been invoked to explain the olivine-rich rocks at the base of S-shaped sills. Settling of phenocrysts or newly formed phases is the most traditionally cited mechanism to produce large concentrations of olivine at the bottom of igneous bodies (Wager & Brown, 1968; Gray & Crain, 1969; Fujii, 1974; Frenkel' *et al.*, 1988, 1989; Marsh, 1988, 1989). The hydrodynamic migration of phenocrysts away from the margins of the intrusion during flow is considered to result in olivine-poor margins whereas gravity aids the production of the abrupt transition between picrite and olivine-poor overlying rocks (Simkin, 1967). The occurrence of basal reversals, upper picrite units and especially a relatively sharp contact between picritic and gabbroic units in the sills of the Noril'sk region are usually taken as evidence for their formation by two- or multiphase injection of distinct melts (Rogover, 1959; Smirnov, 1966; Ivanov *et al.*, 1971; Czamanske *et al.*, 1994, 1995) or emplacement of immiscible basic and picritic melts (Marakushev *et al.*, 1982; Ryabov, 1992). Similar features in basic alkaline sills have also been attributed to multiple emplacement of compositionally distinct, but genetically related magmas (Gibson & Jones, 1991; Gibb & Henderson, 1996; Foland *et al.*, 2000). Recently, Tait & Jaupart (1996) have shown that S-shaped profiles in sills could also be produced by the convective flux of refractory components into a crystal–liquid mush within a boundary layer in the course of *in situ* differentiation of phenocryst-poor magma.

The most common explanation for the origin of sills with D-shaped profiles is flow differentiation involving

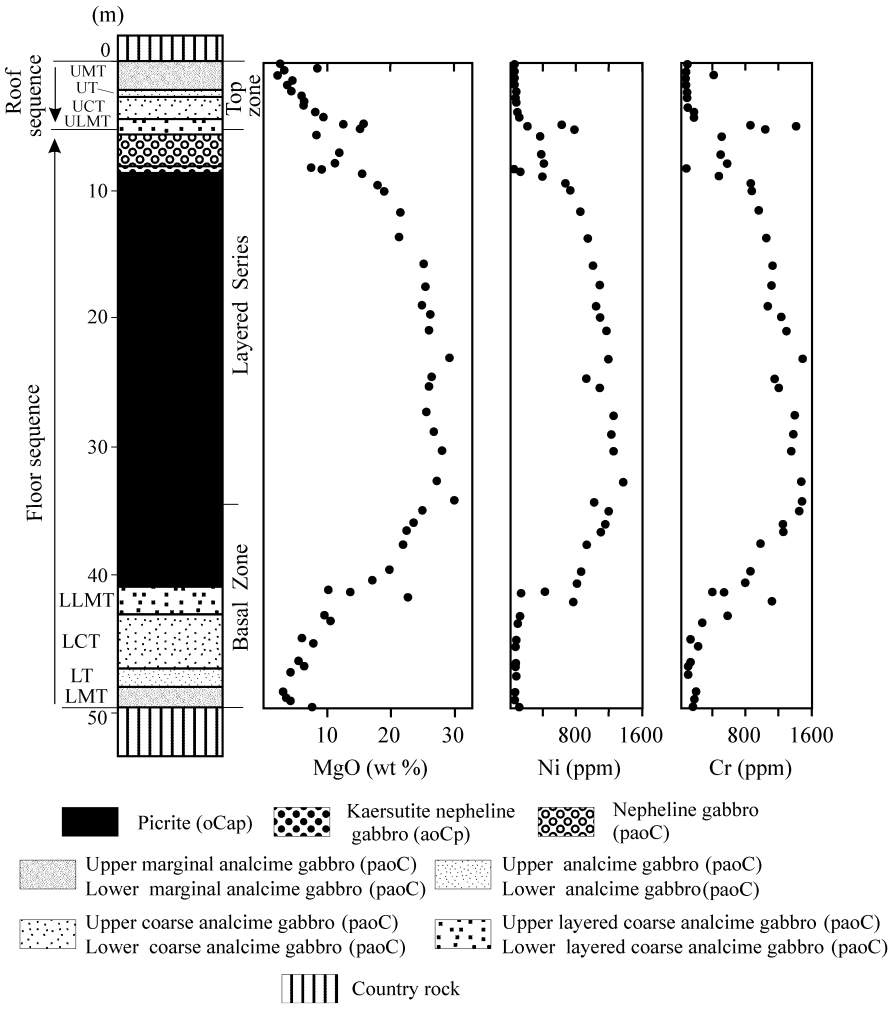

Fig. 5. Generalized stratigraphic section through the Lugar sill (Scotland) showing a D-shaped profile in whole-rock MgO, Cr and Ni contents. Based on Henderson & Gibb (1987). It should be noted that the uppermost four units are mirror images of the bottom four. The identification of cumulate types is based on the petrographic descriptions of Henderson & Gibb (1987). Intercumulus nepheline, analcime, kaersutite and biotite are present in most rocks but are omitted in cumulate abbreviations for simplicity. Thin chilled margins composed of analcime gabbro are not shown.

the segregation of heavy particles (phenocrysts) towards the centre of the flow—the Bagnold effect (e.g. Gunn, 1966; Simkin, 1967; Marsh, 1996). The tendency towards D-shaped profiles in sills is also accounted for by magma intrusion in a series of pulses carrying increasingly higher contents of olivine phenocrysts (e.g. Henderson & Gibb, 1987; Gibb & Henderson, 1992).

Only one explanation has so far been proposed for the origin of sills with I-shaped compositional profiles. This involves the injection of phenocryst-poor magma that crystallizes predominantly through the upper and lower solidification fronts, preventing any evolution of the magma because of the capture of all interstitial liquids (Mangan & Marsh, 1992; Marsh, 1996).

Because of space restrictions, it is impossible to present here a detailed discussion of all these published concepts. Brief summaries of some of the main arguments and evidence are presented below, which lead to the conclusion that existing models are not adequate to explain the characteristic features of S-, D- and I-shaped compositional profiles in sills.

Arguments against the formation of sills by crystal settling and flow differentiation

(1) The fact that sills with I-shaped modal profiles can exhibit well-developed S-shaped cryptic profiles in terms of mg-number and trace element variation (Fig. 7) testifies strongly that crystal settling and flow differentiation are not responsible for the formation of S-shaped profiles. Some other physicochemical process must govern the generation of the S-shaped profiles.

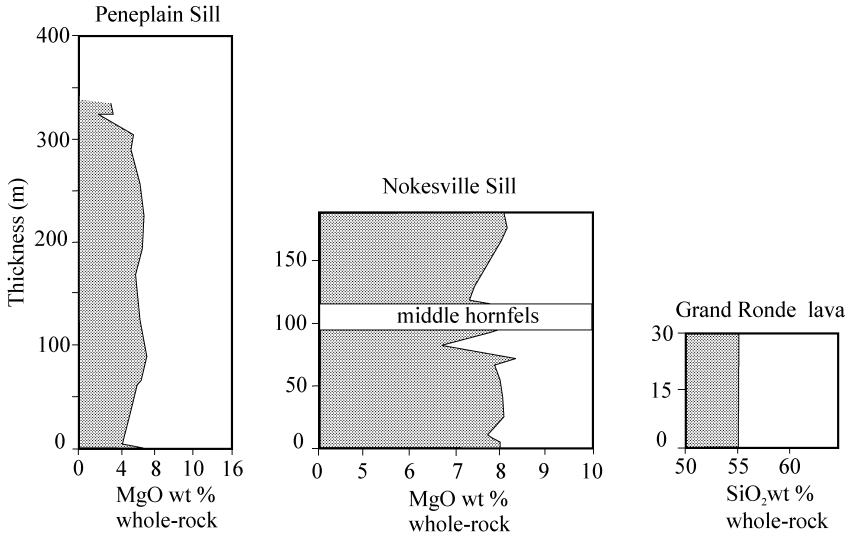

Fig. 6. Compositional profiles in terms of whole-rock MgO and SiO_2 for two I-type sills and a lava flow. The bodies with I-shaped profiles are characterized by little geochemical, petrographic or field evidence for differentiation. They usually do not display either well-developed cumulate zones or late-stage differentiates. Based on the following sources: Peneplain sill, Marsh (1996); Nokesville sill, Froelich & Gottfried (1988); Grand Ronde lava, Mangan & Marsh (1992).

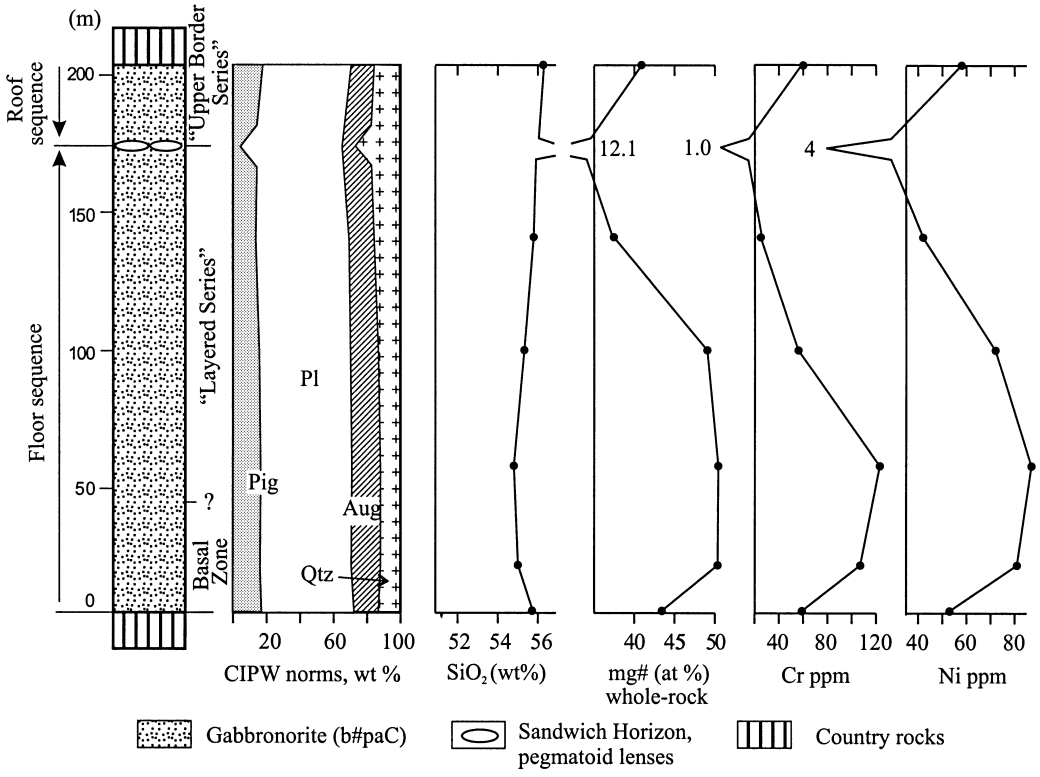

Fig. 7. Generalized stratigraphic section through the New Mountain sill (Antarctica), showing variations in SiO_2 content and normative mineralogy compatible with an I-shaped profile but revealing S-shaped cryptic profiles in terms of whole-rock mg-number, Cr and Ni contents. The data are from Gunn (1966). mg-number = $100Mg/(Mg + Fe^{2+} + Fe^{3+})$.

(2) Neither crystal settling nor flow differentiation can produce adequate separation of orthopyroxene from pigeonite in the Antarctic dolerite sills (Fig. 3), as these minerals have practically the same density. A physicochemical rather than a mechanical process must be responsible for such a regular distribution of pyroxenes.

(3) The occurrence of two maxima in olivine concentration within some sills (Fig. 2d–f) is difficult to reconcile with a gravity-controlled settling crystal model involving a single magma pulse.

(4) Detailed petrographic investigations (e.g. Frenkel' *et al*., 1988; Czamanske *et al*., 1995) show that the Layered Series in sills is primarily composed of cumulates with nearly cotectic mineral proportions. This does not support a crystal settling mechanism, which generally leads to non-cotectic compositions of rocks as a result of appreciable separation of dense crystals from light ones during their gravitational settling to the floor (Morse, 1980).

(5) The roughly cotectic composition of rocks comprising marginal reversals suggests that, in most cases, the intruding magmas were phenocryst poor and consequently cannot produce any appreciable concentration of phenocrysts at the base of the sills (Latypov, 2003).

Arguments against the formation of sills by multiple magma injection

(1) The most impressive evidence for multiple magma injection into sills is the occurrence of pronounced reversals in normal fractionation trends, which are not expected from basic magmas undergoing classical fractional crystallization. Internal contacts between individual units of intrusions that are commonly marked by grain size and textural changes and often interpreted, therefore, as interior chills (e.g. Henderson & Gibb, 1987) provide less reliable evidence for multiple magma injections. This is because the distinct internal contacts can be principally explicable in the frame of a single intrusive episode if the dynamics of magma cooling in the chamber are taken into account (Huppert & Sparks, 1989). The compositional reversals mentioned above are clearly recognized from (a) abrupt changes in the order of phase crystallization and (b) prominent shifts towards less evolved compositions of cumulus minerals. There are numerous documented examples of such reversals in large basic–ultrabasic layered intrusions (e.g. Irvine, 1970; Alapieti, 1982; Todd *et al*., 1982; Faithfull, 1985; Eales & Cawthorn, 1996; Latypov *et al*., 1999*a*, 1999*b*). For instance, a major shift in the crystallization sequence from the Ultramafic Series ($Ol \rightarrow Ol + Opx \rightarrow Opx \rightarrow Opx + Pl \rightarrow Opx + Pl + Cpx$) to the Lower Banded Series ($Ol + Pl \rightarrow Pl + Opx \rightarrow Pl + Opx + Cpx$) is recognized in the Stillwater Complex, testifying that the latter series was formed from a new, distinctly different, magma that was emplaced into the chamber (Todd *et al*., 1982). There is, however, no indication of such compositional reversals at the contact between picritic and gabbroic units in most alkaline (Gibson & Jones, 1991; Gibb & Henderson, 1996; Foland *et al*., 2000) and picrite–gabbro-dolerite sills (Duzhikov & Distler, 1992; Czamanske *et al*., 1994, 1995). They are also absent at the contact between norite and gabbro units in dolerite sills from Antarctica (Gunn, 1966). As an illustration, the internal stratigraphy of the Noril'sk-type intrusions is broadly predictable from *in situ* differentiation of a single pulse of basic magma. The overall trend of crystallization correlates well with the following sequence of phase appearance: $Ol \rightarrow Ol + Sp \rightarrow Ol + Pl + Sp \rightarrow Ol + Pl \rightarrow Ol + Pl + Cpx \rightarrow Ol + Pl + Cpx + Opx$ (Likhachev, 1965, 1977; Nekrasov & Gorbachev, 1978; Zen'ko, 1983). The transition from the picritic units to the overlying layered gabbroic series of the Noril'sk sills reveals no indication of reversals, neither in the sequence of phase crystallization nor in mineral compositions.

(2) Convincing arguments against a multiple magma injection model for the alkaline sills of north Skye have been presented by Simkin (1967, p. 64). He pointed out that the 'multiple intrusion of liquids of differing compositions would require initial intrusion of basaltic liquid (basaltic chilled margins) followed, with no significant time lag (absence of interior chilling), by a more basic, perhaps ultrabasic, liquid *at the base of each sill*. A rather delicate mixing of these two liquids would seem necessary to explain the gradational dolerite-to-picrite transitions at the base, a relatively cool part of the sill where abrupt, if not chilled, junctions would seem more likely. However, in the upper central, and presumably hottest, part of the sill the junction is invariably sharp. Addition of a third pulse of basaltic liquid might explain the upper discontinuities, but would require *three separate intrusions in the same time and space sequences throughout all north Skye sills*.' It remains to be added that acceptance of the multiple injection model would require at least three separate intrusions in the same space sequences not only for alkaline sills (nepheline-normative magma), but also for picrite–gabbro-dolerite (olivine-normative magma) and gabbroic sills (quartz-normative magma). This leaves little room for doubt that a model based on accidental events such as multiple magma injection is untenable for the explanation of the features of S-shaped sills that are commonly observed in igneous bodies throughout the world regardless of their parental magma composition.

(3) The fact that some I-type sills, lacking any commonly cited 'evidence' for new magma pulses (basal reversals, sharp contact between lower picritic and gabbroic units and occurrence of upper picritic units), possess S-shaped cryptic profiles (Fig. 7) strongly indicates that the formation of the S-type sills is not necessarily related to multiple magma injection.

(4) The occurrence of numerous S- and D-type sills with chilled margins that are much more evolved than the bulk sill composition is often taken as strong evidence for multiple magma injection (e.g. Simkin, 1967; Froelich & Gottfried, 1988; Czamanske *et al.*, 1995). This stems primarily from the widespread notion that a single homogeneous liquid should yield a chilled margin representative of the bulk composition of the sill. However, a new model for the formation of marginal compositional reversals in sills and layered intrusions (Latypov, 2003) suggests that relatively evolved chilled margins can be produced, even from a homogeneous liquid, by the operation of Soret diffusion along the intrusion margins. The evolved nature of chilled margins, therefore, cannot be regarded as an indisputable argument for the origin of sills by multiple magma injection.

Arguments against the formation of sills by in situ *crystallization*

Whereas *in situ* crystallization in thermal boundary layers is a principal component of the model presented below for the origin of sills with different compositional profiles, this process can be applied successfully only in combination with the process of Soret fractionation (Latypov, 2003). The reasons why an *in situ* crystallization model cannot be employed in the way that it was proposed by Tait & Jaupart (1996) are as follows:

(1) the *in situ* crystallization model is based on the assumption that the chilled margins of intrusions are representative of the composition of the parental magma, which has not experienced fractionation. However, numerous data on sills and layered intrusions show that this assumption is erroneous as the compositions of chilled margins, along with the lower parts of basal zones, are generally much more evolved than the bulk intrusion composition (Latypov, 2003). This apparent lack of mass balance between the chilled margins and the bulk composition of intrusions, which is one of the essential properties of marginal reversals, finds no explanation in the framework of the *in situ* crystallization model.

(2) The *in situ* crystallization model makes no provision for the generation of top compositional reversals that are so characteristic of sills with double-humped compositional profiles (Fig. 2d–f).

A line of attack on the problem of sills with I-shaped compositional profiles

It has been proposed that I-shaped profiles result from the injection of phenocryst-poor magma where crystal growth occurs predominantly within the solidification front, inhibiting differentiation (Mangan & Marsh, 1992; Marsh, 1996). This explanation seems plausible, particularly for thin sills in which the rate of advance of solidification fronts is high enough to hamper the return of interstitial liquid into the main mass of magma. However, in my opinion this is not the main reason controlling the generation of I-type sills. Close examination of the modal and chemical composition of some typical I-type dolerite sills and lava flows indicates that they crystallized along the $Opx + Pl + Cpx + L$ cotectic in the quartz-normative section of the phase diagram *Ol–Cpx–Pl–Qtz* (Fig. 8). This gives an immediate answer as to why I-type sills show little modal and major element variation: the four-phase cotectic liquids simply cannot produce either basal one-phase cumulates or a well-developed Layered Series. In principle, the entire section of such sills must comprise cotectic pl–pig–aug cumulates (+ intercumulus quartz), closely corresponding to the parental magma composition. Only at the level of the Sandwich Horizon can a minor amount of quartz-rich pegmatoidal material be produced from fluid-rich residual liquid of eutectic composition E_1^4 ($Qtz + Opx + Cpx + Pl = L$). Obviously, the parental magmas for quartz-normative dolerite sills are not the only ones that are able to produce I-shaped compositional profiles. Any magma with a near-eutectic composition can result in the formation of such types of sills. For instance, one can predict that parental magmas close to the eutectic point $Ol + Cpx + Pl + L$ will produce an I-shaped profile with small olivine contents (10–15 vol. %) throughout the entire section of the sill. Olivine-poor sills with a roughly I-shaped modal profile have been reported in the literature (e.g. Gibb & Henderson, 1978; Ryabov, 1992).

PHENOCRYSTS IN SILLS: INTRATELLURIC VERSUS *IN SITU* FORMATION

There is a rather common opinion among petrologists that intratelluric phenocrysts formed at depth before magma intrusion play an important role in the chemical evolution of sills as recorded in their compositional

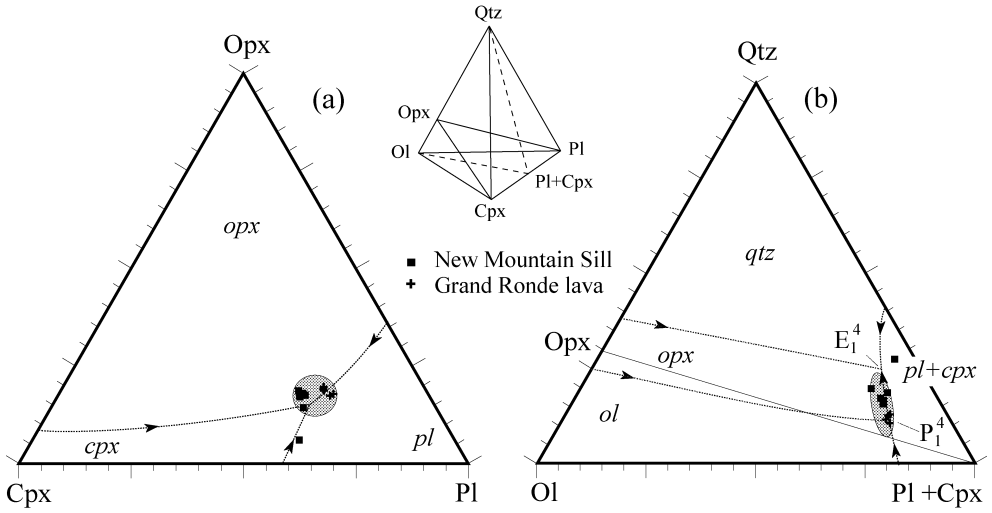

Fig. 8. Two projection planes (a and b) of the isobaro-isoplethic section *Ol–Cpx–Pl–Qtz* showing that all rocks of the New Mountain sill (Gunn, 1966) and Grand Ronde lava (Mangan *et al*., 1986), both characterized by I-shaped modal profiles, are located close to the cotectic line $Opx + Cpx + Pl + L$. This is indicative of near-cotectic compositions for both parental magmas. The crystallization of such cotectic liquids cannot produce either basal one-phase cumulates or a well-developed Layered Series and therefore results in the formation of I-type sills with little modal and major element variation. The position of the two projection planes in the *Ol–Cpx–Pl–Qtz* tetrahedron is also shown. Phase relations along the projection planes are consistent with melt parameters mg-number = 50–75, An = 60–70 and $P < 1$ kbar [slightly modified from Dubrovskii (1998)]. The method of plotting of rock compositions on the projection planes has been given by Latypov (2002). Compositions of the components are expressed in wt %. E_1^4, $Qtz + Opx + Cpx + Pl = L$; P_1^4, $Opx + Cpx + Pl = L + Ol$. Hereafter: E, eutectic point; P, peritectic point; L, melt. Superscripts indicate the number of components involved in the given equilibrium; subscripts show the number of this equilibrium in the system.

profiles (Frenkel' *et al*., 1988, 1989; Marsh, 1988, 1989, 1990, 1991, 1996; Mangan & Marsh, 1992; Chalokwu *et al*., 1993; Czamanske *et al*., 1994, 1995; Ariskin, 1999; Hort *et al*., 1999; Ariskin & Barmina, 2000). Marsh (1996, p. 13) put forward the clearest formulation of this idea: 'no phenocrysts, no post-emplacement differentiation'. In a companion paper (Latypov, 2003) I have suggested, in contrast, that most sills form from phenocryst-poor magmas. I have also noted that the well-developed compositional profiles observed in a number of I-type sills formed from phenocryst-poor magmas are not consistent with the critical role of phenocrysts in magma differentiation. The possible role of intratelluric phenocrysts in the formation of S- and D-type sills requires, however, more detailed examination. There are at least two principal lines of evidence that are taken as indicative of the formation of S- and D-types of sills from parental magmas enriched in phenocrysts. These are the occurrence of intratelluric phenocrysts in the (a) basal and middle cumulate zones of sills and (b) chilled margins.

Phenocrysts in basal and middle cumulates

Phenocryst sizes

Marsh (1996) has reported that many basaltic sills of varying sizes contain dense accumulations of large (2–10 mm) olivine or orthopyroxene phenocrysts near the base (S-type sills) or in the middle (D-type sills). He also suggested on theoretical grounds that such anomalously sized phenocrysts alone precludes them from having grown *in situ*. To explore this issue I have compiled crystal size data from many literature sources that cover approximately 400 basic–ultrabasic sills (Table 1). At least three points are evident from the examination of this table.

(1) Crystal sizes throughout the I-type Peneplain, Ivanovskii, Mikado, Tasmanian and Dæmmevands sills, which are reported to have formed from phenocryst-free or phenocryst-poor magmas, reach 1–3 mm, and in some cases attain 4–12 mm.

(2) Crystal sizes in rocks of S- and D-type sills that were undoubtedly formed *in situ* from a late-stage evolving melt (pyroxenite, gabbro, dolerite, diorite, analcime gabbro) can reach 3–6 mm (e.g. Basistoppen sill), and in some cases 10–15 mm (e.g. Koli sill, Pechenga intrusions).

(3) Crystal sizes of olivine, orthopyroxene and clinopyroxene from the basal or middle cumulate zones of most S- and D-type sills vary from 0·1 to 3 mm. The only exception seems to be the York Haven section of the York Haven sill, where orthopyroxene is reported to attain 5–10 mm.

The main conclusion that can be drawn from the available data is that crystals in basal and middle cumulate zones in most S- and D-type sills are commonly < 3 mm in size. Formation of crystals of such size, on

Table 1: Crystal sizes in basal and middle cumulates of I-, S-, and D-shaped mafic sills

Sills	Type	Thickness (m)	Rocks	Main minerals	Grain size (mm)	Reference
Peneplain sill, Antarctica	I	330	dolerite	pl	0·4–1·0 (Gunn)	Gunn, 1962;
				pl	up to 2·5 (Heyn *et al.*)	Heyn *et al.*, 1995
				cpx, pig	0·4–1·0 (up to 4) (Gunn)	
Ivanovskii sill	I	50	dolerite (middle of the sill)	pl, cpx, pig	0·8–12·0 (for all minerals)	Sinitsin, 1965
Mikado Mountain sill, East Greenland	I	90	dolerite	ol, cpx, pl	0·2–2·0 (for all minerals)	Gisselø, 2001
Tasmanian dolerite sill	I	300	quartz dolerite	cpx	1·1–2·1 (up to 5·0)	McDougall, 1962
				pl	0·4–0·7	
			fayalite diorite	ol	1·1–2·9 (up to 5·0)	
				cpx	1·0–2·0	
				pl	0·6–0·75	
Dæmmevands sill, East Greenland	S	87	dolerite	ol, cpx, pl	0·2–2·0 (for all minerals)	Gisselø, 2001
Siberian dolerite sills, Russia (~10 sills)	S	100–150	poikilitic picrodolerite	**ol**	**0·3–1·5**	Frenkel' *et al.*, 1988
			poikilo-ophitic dolerite	ol	0·2–0·5	
				pl	0·3–0·6	
				cpx†	up to 10·0	
			gabbro–dolerite	ol	3·0–4·0	
				pl	1·5–2·0	
				cpx	0·7–1·0	
Noril'sk type intrusions (Siberia, Russia) (~20 intrusions)	S, D	50–300	picritic, olivine and olivine-bearing gabbrodolerite	**ol**[1]	**0·5–3·0**	Czamanske *et al.*, 1995
				ol[2]	0·1–7·0	
				pl[1]	**>2·0**	
				pl[2]	>0·8	
				cpx[2]	1·0–6·0	
Shiant Isles Main sill, Skye, Scotland	S, D	170	picrite	**ol**	**0·3–2·0**	Gibb & Henderson, 1989, 1996
				pl†	over 10·0	
				cpx†	over 10·0	
			picrodolerite	**ol**	**up to 2·5**	
				pl	0·9	
				cpx†	up to 15·0	
			analcime gabbro	ol†(?)	up to 10·0	
				pl	up to 1·5	
				cpx	up to 3·0	
Lugar sill, SW Scotland	D	49	nepheline gabbro	**ol**	**up to 3·0**	Henderson & Gibb, 1987
				pl†	1·5	
				cpx†	0·1–0·4	
			picrite	**ol**	**up to 1·5**	
				cpx†	up to 1·5	
Little Minch Sill Complex, Skye, Scotland	S	30–150	picrite	**ol**	**2·0–2·5** (up to 5·0)	Gibson & Jones, 1991 (fig. 9)
			picrodolerite	ol	2·0	
				pl	0·5–1·5	
				cpx†	1·5	
			analcime gabbro	ol	3·5	
North Skye sills, Scotland (7 sills)	S	15–100	picrite	**ol**	av. **0·5–0·7**	Simkin, 1967 (fig. 3.8)
			picrodolerite	ol	av. 0·5	
			analcime gabbro	ol	av. 0·25	

Table 1: continued

Sills	Type	Thickness (m)	Rocks	Main minerals	Grain size (mm)	Reference
Koli sill, Finland	S	330	wehrlite	**ol**	**0·1–1·0** *(av. 0·5)*	Vuollo, 1988
			olivine and magnetite pyroxenite	cpx	0·5–3·0 (av. 1·5)	
			magnetite gabbro	pl	0·5–4·0 (av. 2)	
			(lower part)	cpx	0·5–4·0 (av. 1·5)	
			magnetite gabbro	pl	1–10 (av. 3–4)	
			(upper part)	cpx	0·5–15 (av. 4–5)	
Pechenga gabbro–wehrlite intrusions, Russia (~300 intrusions); data for a Pilgujärvi intrusion	S	50–600	wehrlite	**ol**	**0·5–1·0** *(up to 2·0)*	Smolkin, 1977
			olivine pyroxenite	ol	0·2–0·6 (up to 1·0)	
				cpx	0·5–1·5 (up to 3·5)	
			gabbro	pl	0·3–10·0	
				cpx	0·2–10·0	
Kammikivi sill	S	40	peridotite	**ol**	**0·2–1·0**	Hanski, 1992
			pyroxenite	cpx	0·5–1·5	(figs 29 and 31)
Dundonald sill, Ontario	S	750	peridotite	**ol**	**1·0**	Naldrett & Mason, 1968
Chukotat group of sills, Cape Smith Foldbelt of Ungava, Quebec (abundant in the area)	S	100–500	peridotite	**ol**	**0·4**	Bédard, 1987
			pyroxenite	ol	0·7	
				cpx	0·3–1·5	
			gabbro	cpx	0·3–4·0	
				pl	0·8–4·0	
Boston Creek ferropicrite sill or flow, Ontario	S	90	peridotite	**ol**	**1–3**	Stone *et al.*, 1987, 1995
			gabbro	cpx	1–10	
				pl	0·5–3·0	
Shonkin Sag laccolith, Montana	S	70	shonkinite	**cpx**	<**3·0**	Marsh, 1998
Basement sill, Antarctica	S, D	250	pigeonite gabbro	pig	1·5	Gunn, 1962; Hamilton, 1965;
			(base zone)	cpx	1·5	Marsh & Wheelock, 1994
				pl	0·2	
			norite	**opx**	**1–2** (Hamilton)	
					1–3 (Gunn)	
					1–8 (Marsh & Wheelock)	
			pigeonite gabbro	pig	1–3	
			(roof zone)	cpx	1–3	
				pl	0·1–1·0	
York Haven diabase sheet, Pennsylvania	S, D	330–675	bronzite cumulates	**opx**	**5–10** (York Haven section)	Mangan *et al.*, 1993
				opx	**1–3** (Goldsboro section)	
				opx	<**3** (Reesers Summit section)	
Basistoppen sill, East Greenland	I, S	660	picrite	**ol**	**1–2**	Naslund, 1989
			opx gabbro	cpx	1–2	
				opx†	up to 10	
				pl	2–3	
			pigeonite gabbro	pl	3–5	
				cpx	1–3	
				pig	1–4	
			fayalite diorite	ol	up to 5	
				cpx	up to 5	
				pl	up to 6	

Sills	Type	Thickness (m)	Rocks	Main minerals	Grain size (mm)	Reference
Karroo dolerite, Namibia	D	80–110	dolerite (middle	**ol**	**0·2–1·5**	Richardson, 1979
			of the sill)	**pl**	**2–3**	
				cpx	**2–3**	
Palisades sill, New Jersey	S	340	olivine-rich dolerite	**ol**	**0·1–0·3**	Gorring & Naslund, 1995
				cpx	0·3–0·6	
				pl	0·3–0·8	

*Most minerals are cumulus.
†Intercumulus minerals.
Potential intratelluric phenocrysts from basal and middle cumulates of sills are shown in bold type. For Noril'sk type intrusions ol^1 and pl^1 are intratelluric phenocrysts formed in the magma before intrusion, whereas ol^2, pl^2 and cpx^2 are *in situ* phenocrysts. Data for the table are taken from texts and/or photomicrographs of reference papers. av., average size.

the basis of theoretical calculations (Marsh, 1996) and observations on sills formed from phenocryst-free magmas (Table 1), does not require pre-eruption growth. Crystals can attain such size by *in situ* growth in sills. This means that the basal and middle cumulates in basic–ultrabasic sills can be principally produced *in situ* from phenocryst-poor or even phenocryst-free parental magmas. In addition, the data show that crystals that grow in sills during the middle and late stages of magma differentiation can attain 10–15 mm. This suggests that the 2–10 mm size limit theoretically proposed for the identification of intratelluric phenocrysts in sills (Marsh, 1996) needs to be reconsidered.

Phenocryst size/frequency variations

Strong evidence for the existence of two generations of crystals (intratelluric and *in situ* phenocrysts) in sills would be a discovery of bimodal crystal size populations. Wyllie & Drever (1963) and Gibb (1968) have carried out such investigations of olivine size distribution in small picritic intrusions of the Isle of Skye, Scotland. Both studies have shown that these intrusive bodies have a continuous gradation in the size of olivine rather than two distinct size groups. These results do not completely preclude the existence of two generations of olivine crystallization, however, because bimodal distributions can fail to occur if olivine of a second generation is deposited on the surfaces of first generation crystals in addition to forming new crystals (Gibb, 1968). It is important, however, to note that the lack of bimodal size distribution does not, at least directly, support the idea of the existence of two generations of crystals in sills.

Phenocryst morphology

Czamanske *et al.* (1995) carried out perhaps the only detailed investigation of the morphology of phenocrysts throughout sill sections. They presented convincing evidence for the existence of two morphologically different generations of olivine in Noril'sk type intrusions. The first-generation olivine, having a mainly idiomorphic form and containing no inclusions of other minerals, occurs solely in the picritic units of the intrusions and is identified as intratelluric phenocrysts. The second-generation olivine is represented mainly by (1) large oikocrystic or xenomorphic grains, containing, or being penetrated by, laths and microlites of plagioclase and (2) small to very small, rounded and idiomorphic grains, which are common only in the gabbroic units of the intrusions and are identified as an *in situ* type of phenocryst. Although such a subdivision of morphologically different olivines into products of intratelluric and *in situ* stages of crystallization is possible, it is certainly not the only explanation. It is conceivable that both morphological generations of olivine are produced *in situ*. The first-generation olivine in the picrites crystallized as a sole liquidus phase while the parental magma fractionated through the primary volume of olivine. This is why this olivine contains no inclusions of other minerals. The second-generation olivine crystallized during liquid fractionation along an $Ol + Pl + L$ cotectic (Ol 15%, Pl 85%) and at an $Ol + Pl + Cpx + L$ eutectic point (Ol 10%, Pl 60%, Cpx 30%) where olivine is a modally subordinate phase. Nucleation and crystallization of olivine here can be suppressed by that of modally predominant plagioclase and clinopyroxene. This can explain why the second-generation olivine contains, or is penetrated by, crystals of plagioclase.

Phenocrysts in chilled margins

Porphyritic texture

The observation that crystals of two distinct average sizes (phenocrysts and groundmass crystals) are

present in chilled margins is traditionally interpreted by petrologists in terms of a two-stage cooling history imposed by external factors. It is commonly supposed that the phenocrysts form slowly at depth whereas the groundmass forms on 'quenching' against cold country rocks. It became, however, clear from experimental studies on lunar samples that the two-stage crystallization implicit in a porphyritic texture does not necessarily imply a two-stage cooling history. It was demonstrated that a porphyritic texture could develop from single-stage cooling of basaltic liquids both at constant linear and decreasing nonlinear cooling rates (e.g. Lofgren *et al*., 1974; Walker *et al*., 1976; Lofgren, 1980). In particular, a bimodal grain-size distribution of pyroxene was obtained during single-stage cooling in all the dynamic crystallization experiments as well as the natural rocks. The necessary condition for the formation of a porphyritic texture is when the liquidus or near-liquidus phase(s) (olivine or pyroxene) are modally dominant and have a significant temperature interval of crystallization (up to 30°C) before the appearance of another liquidus phase. In this case, as the liquid cools, the first generation of olivine (or pyroxene) nucleates and grows, without competition from other crystallizing phases, to typical phenocryst size (Lofgren, 1980). Upon reaching a cotectic line a new groundmass generation of smaller olivine (or pyroxene) and plagioclase starts to form although the precise mechanism of its production remains obscure (Dowty, 1980). Formation of the first generation of phenocrysts can be facilitated by a small amount of nuclei of submicron size ranges present upon injection of magma in the chamber. The nuclei can represent the unmelted remains of crystalline material that mixed with the magma during transport to the surface. The nuclei can also be formed by homogeneous nucleation during the long pre-emplacement history of the magma (Lofgren, 1983). In general, simple conductive cooling of a magma body that solidifies because of heat loss through its margins seems a suitable environment for the production of a porphyritic texture (Walker *et al*., 1976).

Phenocryst morphology

Drever & Johnston (1957) first postulated that direct growth rather than resorption was responsible for the skeletal development of crystals in chilled margins. They concluded that there was ample evidence to show that large skeletal olivine phenocrysts could form *in situ* from a rapidly cooling magma and that such phenocrysts were not necessarily derived from elsewhere. Later Donaldson (1976) provided strong experimental support for this idea. He also showed that skeletal crystal shapes reflect not a rapid cooling rate, but rather a rapid growth rate caused by the high MgO content of the melt. Skeletal olivines grow at much slower cooling rates in high-MgO melts (picrites) than in more MgO-poor melts (basalts). On this basis, abundant hopper olivine in the porphyritic picritic minor intrusions of the Scottish and West Greenland Tertiary igneous provinces has been interpreted as an *in situ* phenocryst phase (Donaldson, 1976).

It should be emphasized that hopper olivine is not the only morphological type of olivine phenocryst that can form at sill margins. The hopper olivine in olivine-normative basalt forms at a relatively high cooling rate of ~2·7–15°C/h; subhedral and granular olivine grows at $<2{\cdot}7$°C/h (Donaldson *et al*., 1975; Donaldson, 1976). Cooling at such relatively slow rates is estimated to take place at the margins of small dykes and lava flows (Baker & Grove, 1985; Kretz *et al*., 1985). Hence it would be incorrect to think that relatively rapid cooling near the chilled margins of sills will almost certainly produce skeletal olivine (e.g. Gibb, 1968, 1972). The predominance of granular and scarcity of skeletal olivine phenocrysts in the chilled margins of some basic–ultrabasic sills suggests that the cooling rate was $<2{\cdot}7$°C/h. An important factor in the formation of granular rather than skeletal phenocrysts can also be a small amount of nuclei present upon the injection of magma in the chamber. Growth on pre-existing nuclei makes the shapes of liquidus phases less dependent on variations in cooling rate. It was also experimentally demonstrated, by using plagioclase, that initially skeletal crystals can fill in to become tabular with continued growth at a cooling rate of 2°C/h (Lofgren, 1980). This important observation presents a real mechanism for how skeletal crystals can be readily transformed into granular ones leaving little trace of the initial crystal morphology. A much longer time period for crystallization of chilled margins in comparison with laboratory experiments, as well as crystallization of natural magmas under conditions of fluid pressure that significantly increase the rate of chemical diffusion, suggest that such a morphological transformation is possible.

An additional explanation for the rare occurrence of skeletal minerals in chilled margins comes from the experimental work of Kouchi *et al*. (1986). They have shown that stirring, or shear flow, during crystallization, dramatically changes both the nucleation rate and crystal morphology of plagioclase and clinopyroxene compared with experiments under static conditions. At amounts of supercooling >45°C, stirring increases the nucleation rate by ~10 times and skeletal crystal morphologies are never observed. Thus the rare occurrence of skeletal crystals in the chilled margins of sills may also indicate that crystallization

takes place during continuous magma flow that is provided by vigorous thermal convection in the chamber. A similar explanation has been adopted for the interpretation of the texture of quench rocks between macrorhythmic units in the Kap Edvard Holm gabbro complex (Tegner *et al*., 1993). Overall, it is clear from the above discussion that ample opportunities exist in nature for *in situ* growth of subhedral rather than skeletal crystals during the cooling of sill margins.

Phenocryst sizes and abundances

Tables 2 and 3 present a compilation of data on the shapes, sizes and abundances of phenocrysts observed in the chilled margins of sills and in slow-rate cooling experiments, respectively. Close examination of the data shows that crystal shapes (from hopper to granular) and sizes (up to 1–2 mm, with the exception of 6–7 mm long skeletal crystals) that have been attained at a cooling rate of 2–3°C/h are comparable with those documented in chilled margins. Thus, one can conclude that the size and shape of crystals is not always a criterion of critical significance in deciding whether or not their precipitation ante-dated or post-dated magma intrusion. There seems therefore to be no strong obstacle to the suggestion that most phenocrysts observed in chilled margins can be produced *in situ*. The total amount of phenocrysts in chilled margins, judging from the abundance of *in situ* formed hopper phenocrysts in the Chukotat group of sills, Quebec (Table 2), can reach as much as 10–40 vol. %.

Phenocryst composition

I am unaware of any studies presenting compositional criteria for distinguishing intratelluric phenocrysts from those formed *in situ* in chilled margins. It is reasonable to expect that the inner zones of true intratelluric phenocrysts are characterized by the highest mg-number (ol, opx, cpx) and An contents (pl) and show relatively smooth zoning profiles, whereas the outer parts of the phenocrysts, which are contemporaneous with the groundmass, will become more evolved towards the crystal margins. Analysis of experimental data shows, however, that similar compositional features can be attained by *in situ* phenocryst growth at a low rate of cooling. In particular, Walker *et al*. (1976) did not observe any decrease in the Fo content of the cores of olivine as a function of cooling rate (0·5–2000°C/h), temperature (1325–600°C), and pressure (0–12 kbar) for a constant bulk composition. Also, Grove & Bence (1977) failed to find any evidence of major element zoning in pyroxene, caused by cooling rates up to 150°C/h. Both observations were attributed to heterogeneous nucleation of minerals on Fe-metal particles present in the melt as a result of the iron-capsule technique employed (Lofgren, 1980). Thus, if as was suggested above, *in situ* phenocrysts in chilled margins nucleate and grow on pre-existing nuclei, then the core compositions will be hardly distinguishable from those of intratelluric phenocrysts. Compositional zoning also seems a poor guide for distinguishing intratelluric from *in situ* phenocrysts. Donaldson *et al*. (1975) reported no zoning in an olivine from a 2·7°C/h cooling rate experiment, suggesting that equilibrium is achieved at such a cooling rate. Lofgren *et al*. (1974) and Grove & Bence (1977) found that at cooling rates <3°C/h, olivine had time to react with the liquid to form pyroxene as the equilibrium phase relations suggest. At a cooling rate of $\sim$2°C/h the inner third to half of the plagioclase crystals show little zoning and only the outer portion is zoned (Lofgren, 1980). Thus there seems to be no reliable compositional criterion that would permit one to distinguish intratelluric phenocrysts from those formed *in situ*.

Concluding remark

The size, morphology and composition of phenocrysts in the basal and middle cumulates as well as in the chilled margins of sills present no compelling evidence for their intratelluric origin. It is conceivable that most of these phenocrysts actually form *in situ*. Those phenocrysts that are distinguished by especially large sizes could indeed represent intratelluric fractions of phenocrysts. In most cases, however, their amount is unlikely to exceed a few percent.

A PROPOSED *IN SITU* CRYSTALLIZATION MODEL FOR THIN SHEET-LIKE MAGMA BODIES

It follows from the above and a companion paper (Latypov, 2003) that current models of magma differentiation in the high-level magma chambers do not provide an adequate explanation for the origin of the different compositional profiles observed in sills. The obvious question is: What mechanism can resolve the problem? A close look at this problem yields the conclusion that the best candidate is an *in situ* crystallization model. There are several variants of this model (e.g. Campbell, 1978; McBirney & Noyes, 1979; Cawthorn & McCarthy, 1980, 1985; Sparks *et al*., 1984; Langmuir, 1989; Marsh, 1989; Nielson & De Long, 1992). I favour one of the most advanced variants that was developed by Jaupart & Tait (1995) and Tait & Jaupart (1996). As previously noted, however,

Table 2: Shape, sizes and amount of phenocrysts in the chilled margins of mafic sills

Sills	Thickness (m)	Minerals	Shape	Size (mm)	Total amount (%)	Reference
Picritic intrusions, Scotland and West Greenland	0·2–9·0	ol	hopper, anhedral, skeletal	0·5–2·5 up to 6	10–15	Drever & Johnston, 1957, 1958
Picrite sill, Hebrides	1·8	ol	anhedral, elongate hopper	0·1–2·0	10–15	Wyllie & Drever, 1963 (text-fig. 2)
Picritic sheet, Skye, Scotland	1·4	ol	subhedral, rare skeletal	up to 1·5–2·0	17–22.5	Gibb, 1972
Little Minch Sill Complex, Skye	30–150	ol	euhedral, subhedral, hopper	0·3–2·0		Gibson & Jones, 1991 (fig. 9)
Shiant Isles Main sill, Skye	170	ol	skeletal, anhedral, irregular or euhedral	up to 2·0		Drever & Johnston, 1957 (text-fig. 16)
North Skye sills, Scotland (Tuath, Skudiburgh, Kilmuir)	15–100	ol		av. 0·25–0·5	10–20	Simkin, 1967 (fig. 3.8)
Chukotat group of sills, Cape Smith Foldbelt of Ungava, Quebec	100–500	ol	hopper	0·4	10–40	Bédard, 1987
Noril'sk type intrusions, Siberia, Russia	50–300	ol	clutch (paw-like)	1·0–7·0	10–15	Likhachev, 1994; Czamanske *et al.*, 1995
			(skeletal?) rounded	0·1–0·4		
		pl	prismatic	0·7–4·0		
York Haven diabase sheet, Pennsylvania	330–675	pl		1·0	6	Mangan *et al.*, 1993
		cpx		1·0		
Basistoppen sill, Greenland	660	pl		0·3–0·5		Naslund, 1989
Basement sill, Antarctica	250	pl	anhedra	$<$0·5	3	Hamilton, 1965
Tasmanian sills	300	opx		0·2–0·5	5	McDougall, 1962
		cpx		0·08		
		pl		0·1		
Karroo dolerite, Namibia	80–110	ol	euhedral	0·2–1·2	23	Richardson, 1979
		aug	euhedral (glomerocrysts)	0·1–0·4		
		pl		2–5		

*Data for the table are taken from texts and/or photomicrographs of reference papers.

Table 3: Shape and sizes of phenocrysts at low rate cooling experiments

Composition	Cooling rate (°C/h)	Minerals	Shape of grains	Size (mm)	Reference
Olivine-normative basalt (Apollo 12)	3	ol	hopper	0·7	Donaldson, 1976, fig. 9
Olivine-normative basalt (Apollo 12)	2·7	ol	subsequent, euhedral, internally skeletal	up to 6·0*	Donaldson *et al.*, 1975
		cpx	subhedral, subsequent	up to 3·5*	
		pl	elongate skeletal laths	up to 1·0*	
Feldspathic basalt	2	pl	tabular, somewhat skeletal	1–2	Lofgren, 1977
High-titanium basalt	2	ol	equant skeletons	2	Usselman *et al.*, 1975, fig. 3, table 4
		cpx	euhedral equant	0·5	
Quartz-normative basalt	2·5	cpx	euhedral equant	0·5–1·0	Lofgren *et al.*, 1975, fig. 3
An_{40}–H_2O melt	2	pl	tabular	1–2	Lofgren, 1980, fig. 7

Data for the table are taken from texts and/or photomicrographs of reference papers.
*A rate of cooling at which these crystal sizes have been attained is not specified in the text of a reference paper.

this variant does not provide a reasonable interpretation for the origin of marginal compositional reversals in sills. To overcome this drawback I have attempted to modify the *in situ* crystallization model by including the effect of Soret fractionation to account for the formation of compositional reversals in sills (Latypov, 2003).

The basic principles of the model can best be illustrated by considering a sill with a double-humped compositional profile. For the sake of convenience let us take a basic–ultrabasic sill (Fig. 9a) whose parental magma composition X′ lies in the primary olivine phase field in a simple silica-undersaturated system *Ol–Pl–Cpx* (Fig. 9b). The trend of crystallization of the parental magma X′ can be readily traced in the phase diagram as shown by the letters located along the compositional profile for whole-rock mg-number, Cr and Ni (Fig. 9a). The model suggests that the sill is principally composed of floor and roof sequences that meet at the level of the Sandwich Horizon (Fig. 9a). The floor sequence of the sill is proposed to comprise the Basal Zone and the Layered Series, whereas the roof sequence contains the Top Zone and Upper Border Series. The lines of demarcation between the coupled units of the floor and roof sequences run through the lower and upper crossover maxima (Latypov, 2003) exhibiting the most primitive mineral and rock compositions in the entire section of the sill. The maxima do not coincide with any lithological boundary, being located completely within the modally homogeneous dunite layers, and hence can be identified only with the help of mineral compositional data. The Layered and Upper Border Series are composed of the lithological succession dunite, troctolite and olivine gabbro, which is strictly consistent with the expected trend of crystallization of the parental magma X′: $Ol \rightarrow Ol + Pl \rightarrow Ol + Pl + Cpx$. The Basal and Top Zones consist of the succession olivine gabbro, troctolite and dunite, showing the trend of crystallization $Ol + Pl + Cpx \rightarrow Ol + Pl \rightarrow Ol$, which is the exact opposite of that of the parental magma X′. The Basal and Top Zones, being mirror images of the Layered and Upper Border Series sequences, respectively, are therefore referred to as basal and top reversals.

The whole scenario for the formation of the sill with the double-humped compositional profile is subdivided into eight principal stages T_1–T_8 (Fig. 10), which are presented below.

Stage T_1: chilled margin remelting

The emplacement of the first batch of fluid-saturated phenocryst-free or phenocryst-poor magma X′ into cold country rock leads to the immediate formation of a chilled margin corresponding compositionally to the initial parental magma. The initial chilled roof margin, however, can subsequently be partly or completely melted back when heat flux from the vigorously convecting magma in the chamber becomes equal to or exceeds the conductive heat flux in the country rock (Huppert & Sparks, 1989). Remelting of a chilled margin at the floor is considered to be less effective but can still occur by magma flow through the chamber in which heat is advected to both boundaries (Huppert & Sparks, 1989). A common lack of mass balance between the chilled floor margins and bulk compositions of sills is taken as an indication that their marginal

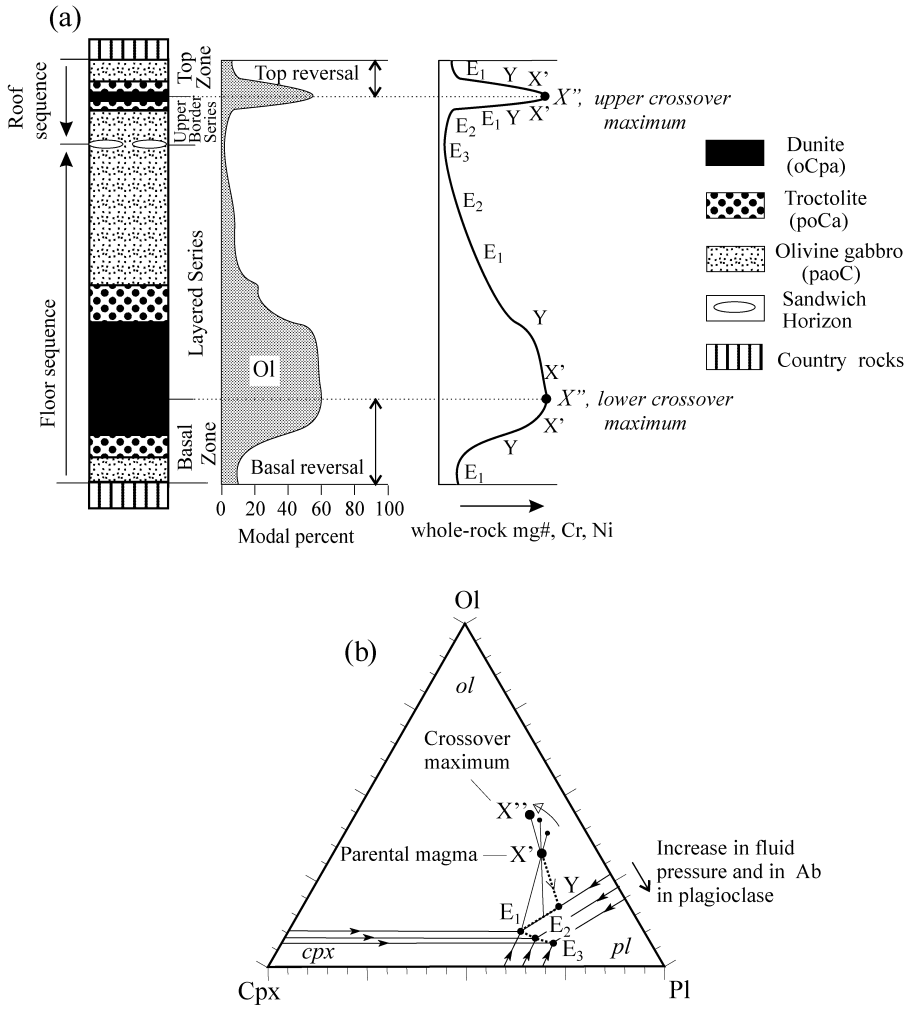

Fig. 9. A hypothetical basic–ultrabasic sill with a double-humped compositional profile (a). The sill is composed of floor and roof sequences that converge at the Sandwich Horizon. The floor sequence comprises the Basal Zone and Layered Series, whereas the roof sequence contains the Top Zone and Upper Border Series. The Basal and Top Zones represent the condensed compositional mirror images of the Layered and Upper Border Series, respectively, and are therefore referred to as basal and top reversals. The trend of crystallization of the parental magma X′ (b) can be traced using a silica-undersaturated system *Ol–Pl–Cpx* and letter abbreviations along the compositional profile of whole-rock mg-number, Cr and Ni in (a). The rock succession dunite, troctolite and olivine gabbro in the Layered and Upper Border Series is consistent with the expected trend of crystallization of the parental magma X′: $Ol \rightarrow Ol + Pl \rightarrow Ol + Pl + Cpx$. The trends of crystallization in the basal and top reversals are exactly the opposite. The lower and upper crossover maxima (X″) marking the interior boundaries of the basal and top reversals exhibit the most primitive composition of minerals and rocks observed in the entire section of the sill. These arise as a result of progressive removal of low melting fractions from the initial composition X′ while it crystallizes the basal and top reversals along the path $E_1 \rightarrow Y \rightarrow X'$ (b). It should be noted that the magma at the crossover maxima (X″) is more primitive but not hotter than the parental magma (X′). Progressive contraction ($E_1 \rightarrow E_2 \rightarrow E_3$) of the plagioclase field as a result of an increase in fluid pressure and albite content of plagioclase during liquid fractionation is also shown. (See text for further discussion.)

facies usually form after prolonged and extensive melt-back of the initial chilled floor (Latypov, 2003).

Stages T_2–T_4: basal and top reversal formation

The formation of basal and top reversals takes place through the non-equilibrium evolution of liquid boundary layers as a result of a temperature gradient imposed by the cold country rock (Latypov, 2003). The boundary layers tend toward a stationary non-equilibrium state that is attained when the compositions of melts in the boundary layers become adjusted to an imposed temperature gradient in accordance with liquidus phase equilibria. To achieve such a compositional adjustment the system transfers high melting point components (HMPC) from the liquid boundary layer into the main magma body and low melting point components (LMPC) in the opposite direction. Mass transfer across the short distance of a

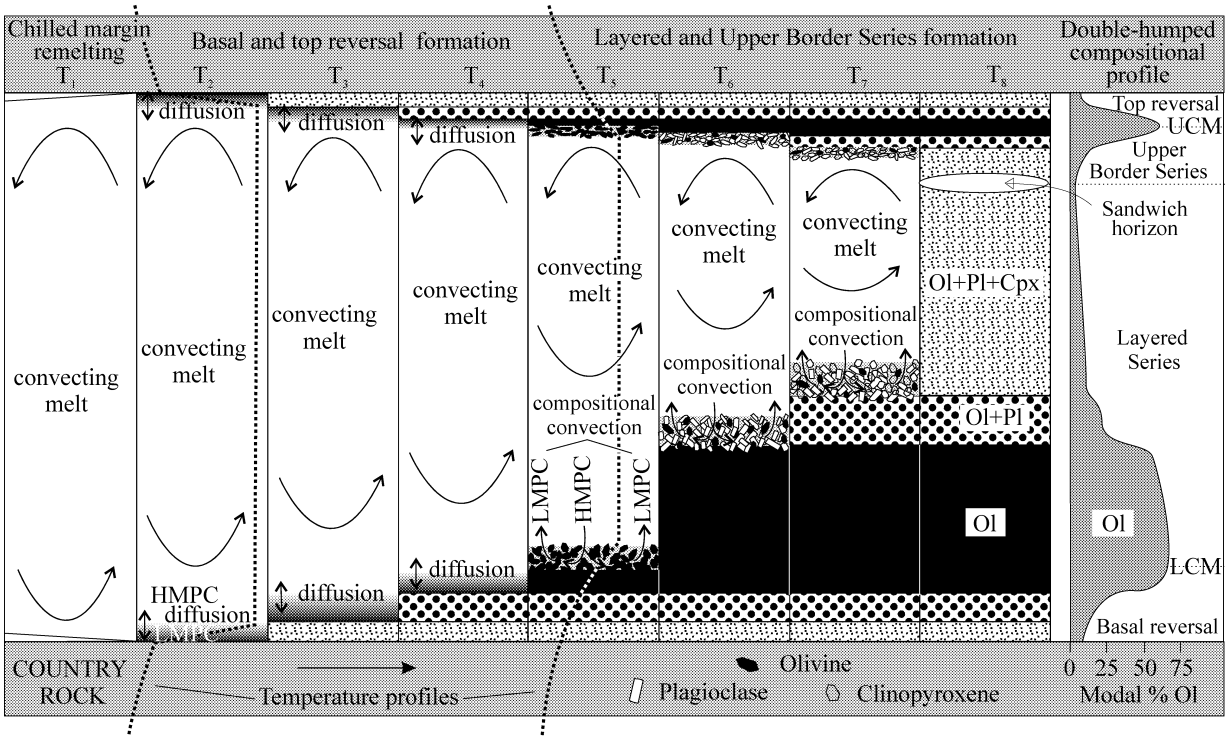

Fig. 10. Successive stages in the formation of a hypothetical basic–ultrabasic sill with a double-humped compositional profile and parental magma composition X′ lying in the olivine field of a silica-undersaturated system *Ol–Pl–Cpx* (Fig. 9). The formation of the sill starts with remelting of the initial chilled margins (T_1) followed by crystallization of basal and top reversals (T_2–T_4) and culminates in generation of the Layered and Upper Border Series (T_5–T_8). The liquid evolution during formation of both reversals is provided by Soret fractionation across the thin thermal boundary layers, aided by vigorous natural convection in the main magma body that continually brings fresh magma to the boundary layers. In contrast, liquid differentiation during generation of the Layered and Upper Border Series takes place by compositional convection in the mushy region of the floor boundary layer, assisted by thermal convection in the main magma body. It should be noted that Soret fractionation aids the transfer of LMPC towards the chamber margins whereas compositional convection brings them towards the interior of the chamber. Thermal convection acts to keep the upper thermal boundary layer thin, thus leading to a thicker rock sequence at the base than at the roof. Two sketches of the temperature field are indicated for stages T_2 and T_5. LMPC, low melting point components; HMPC, high melting point components; LCM, lower crossover maximum; UCM, upper crossover maximum. Other abbreviations as in Fig. 9. (See text for further discussion.)

liquid boundary layer occurs mainly by Soret diffusion, which is aided by thermal convection in the main magma body. Soret fractionation under the initial highest thermal gradient produces a liquid boundary layer comprising, in a stationary state, compositions that span in reverse sequence a nearly entire liquid line of descent of the parental magma X′. Compositional oversaturation in the main magma body that arises as a result of a supply of HMPC from the liquid boundary layer is uniformly distributed throughout the magma chamber via convection. Nucleation and crystallization occurs predominantly in the stagnant lowermost regions of the boundary layers composed of the most evolved liquid compositions. Upon the progressive decrease in magnitude of the thermal gradient related to the growing cumulus pile, and an overall fall in the temperature of the whole magma body, the compositional characteristics of the liquid boundary layers in the stationary state become more and more primitive. Given favourable kinetic conditions, the stagnant crystallizing region of the liquid boundary layers in this process progressively travels all the way along the liquid line of descent of the parental magma.

According to the above predictions, the trend of crystallization of the basal and top Soret-produced liquids should be exactly the reverse of that of the parental magma X′: *Ol* + *Pl* + *Cpx* (E_1, olivine gabbro) → *Ol* + *Pl* (E_1–Y, troctolite) → *Ol* (Y–X′, dunite) (Figs 9 and 10). The crystallization of these liquids will result in clearly pronounced basal and top reversals—mirror images of the future Layered and Upper Border Series. The reversals are distinguished by: (1) an apparent lack of mass balance between the chilled margins composed of olivine gabbro (a eutectic point E_1) and the initial parental magma composition (point X′); (2) the order of phase crystallization; (3) a trend of mineral compositions (whole-rock mg-number, Cr, Ni) opposite to those expected from the fractional crystallization of parental magma X′.

Opportunities for effective Soret fractionation in the liquid boundary layers remain only as long as a high thermal gradient persists locally during thermally juvenile magmatic stages (Lesher & Walker, 1991). Thus, when the thermal gradient in the boundary layers wanes, Soret fractionation will no longer be able to cause magmatic differentiation and its effect will be insignificant. The stratigraphic levels where the Soret effect ceases to be active are referred to as the lower and upper crossover maxima (Fig. 9a, points X″) forming from magma more primitive (but not hotter!) than the parental magma X′. This magma arises as a result of the progressive removal of low melting fractions from the initial composition X′ while the basal and top reversals crystallize along the path $E_1 \rightarrow Y \rightarrow X'$ (Fig. 9b). This is why the crossover maxima represent the most primitive compositions of minerals and rocks observed in the entire sill. Obviously the mineral compositions (e.g. Fo % in olivine) that occur slightly above and below the level of the lower and upper crossover maxima can be reliably used for estimation of the parental magma composition.

It should be noted that the crystallization of magma in the marginal zones of intrusions generally occurs relatively rapidly, as indicated by the common fine- to medium-grained textures of most marginal rocks. Crystallization will therefore proceed without much release of intercumulus liquid from the crystallizing boundary layer into the main magma body so that the interface between solid and melt can be treated here as a nearly flat boundary. However, from the level of the crossover maxima, where rocks are already medium to coarse grained, the interface between solid and melt can no longer be considered flat. At this time the thermal boundary layers are likely to represent a crystal–liquid mush from which, under favourable conditions, interstitial liquids can escape into the main reservoir of the magma.

Stages T_5–T_8: Layered and Upper Border Series formation

Upon reaching the crossover maxima, the formation of the Basal and Top Zones in non-equilibrium conditions gives way to the formation of the Layered and Upper Border Series in equilibrium conditions. Thus the importance of the crossover maxima is that they mark the boundary where a non-equilibrium style of evolution of the magma in the chamber gives way to an equilibrium one. The future evolution of the magmatic system can be fully described in the framework of an *in situ* crystallization model developed in recent publications (e.g. Sparks *et al.*, 1984; Tait *et al.*, 1984; Tait & Jaupart, 1992, 1996; Jaupart & Tait, 1995). The model treats the magma chamber as a central mass of nearly crystal-free convecting magma, which gradually loses heat and crystallizes inwards from its margins. The transition from crystal-free magma in the central part of the chamber to completely solidified rock in the outer parts is thought to occur through a boundary layer of crystal–liquid mush, with the proportion of interstitial liquid decreasing systematically in the direction of falling temperature. The model presumes that the evolved intercumulus liquids within the boundary layer at the floor will be unstable as a result of enrichment in SiO_2 and volatiles, which tend to reduce its density. In most circumstances, this compositional effect dominates the opposing thermal effect so that relatively primitive, denser liquid from the overlying reservoir infiltrates down through the crystalline matrix of the boundary layer, driving out the lighter, more evolved interstitial liquid. It is the transfer of evolved liquid into the overlying reservoir through density-induced compositional convection at the floor that is considered to be the main mechanism by which crystallization at the margins results in differentiation of the magma body as a whole. It is worth noting one apparent difference in the style of component redistribution before and after the crossover maxima. Before the crossover maxima (stages T_2–T_4), liquid differentiation occurs through the flux of LMPC from the interior of the magma body towards the chamber margins, accompanied by flux of HMPC in the opposite direction. After the crossover maxima have been reached, the direction of transfer of LMPC and HMPC is reversed (stages T_5–T_7).

During the formation of the Layered and Upper Border Series the magma in the chamber follows through a normal order of phase appearance $Ol + L$ (X″–Y, dunite) $\rightarrow$ $Ol + Pl + L$ (Y–E_1, troctolite) $\rightarrow$ $Ol + Pl + Cpx + L$ (E_1–E_3, olivine gabbro). This trend is fully compatible with the location of the parental liquid within the primary field of olivine (Fig. 9b). The modal compositions of the rocks are strictly constrained by the topology of the liquidus phase diagram. In this context it should be emphasized that an abrupt compositional transition from dunite (oCpa) to troctolite (poCa) is a consequence of the shift in magma composition from the primary volume of olivine ($Ol + L$) to the olivine–plagioclase cotectic ($Ol + Pl + L$). This cotectic is characterized by the predominance of plagioclase (70–85 wt %) over olivine (15–30 wt %). This is why, after the formation of dunite by exclusive precipitation of Ol within its primary phase volume, the olivine abundance in the overlying troctolite, crystallizing on the $Ol + Pl + L$ cotectic, must drop abruptly to as little as 15 wt % (stage T_6). It is therefore not reasonable to take this common phenomenon as evidence for the formation of the picritic and gabbroic zones of basic–ultrabasic sills from two distinct magmas

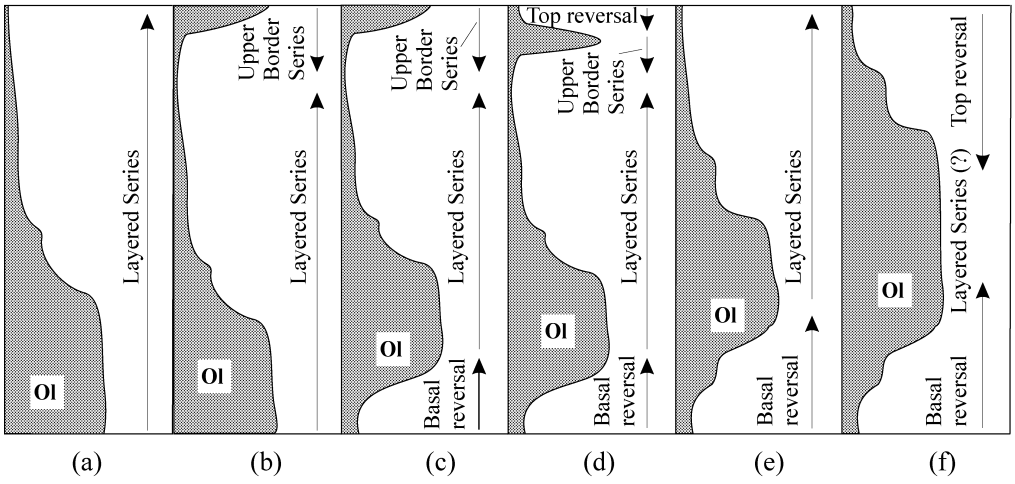

Fig. 11. Different modal profiles (a–f) observed in sills that can be interpreted as a result of different combinations of four principal units—basal reversal, Layered Series, Upper Border Series and top reversal—which were identified in a profile through a hypothetical basic–ultrabasic sill with a double-humped modal profile [Fig. 9 and profile (d)].

(Smirnov, 1966; Ivanov *et al*., 1971; Marakushev *et al*., 1982; Ryabov, 1992; Czamanske *et al*., 1994, 1995). Upon further crystallization, the liquid will reach the eutectic point E_1 where olivine gabbro is produced. Here the proportion of olivine in the phase assemblage falls to 5–10 wt % (stage T_7). Further gradual decrease in the olivine content of olivine gabbro could take place as a result of the progressive contraction of the plagioclase field. The latter can result from increases in fluid pressure (Yoder, 1965) and in the albite content of plagioclase (Bowen, 1915) in the course of liquid fractionation along the path $E_1 \rightarrow E_2 \rightarrow E_3$. The Layered and Upper Border Series, growing contemporaneously from the roof and floor and meeting at the Sandwich Horizon, will exhibit similar trends of phase crystallization. The thickness of the Upper Border Series, however, will be much smaller, as vigorous thermal convection in the main mass of magma will keep the upper thermal boundary layer thinner than the lower one. Thermal convection provides a good explanation for the fact that, in most well-described sills and intrusions, rock sequences that have crystallized from the roof are typically 6–7 times thicker than those that formed at the floor (Jaupart & Tait, 1995).

IMPLICATIONS OF THE PROPOSED *IN SITU* CRYSTALLIZATION MODEL FOR THE ORIGIN OF VARIOUS COMPOSITIONAL PROFILES

The validity of any model can primarily be judged from its ability to explain or/and reproduce actual observations. In this respect the proposed model adequately duplicates the shape of the compositional profile for complex, 'double-humped' sills (compare Fig. 10 with Fig. 2d–f). Significantly, the model can account for the three main features of double-humped sills, namely, the basal reversal, the upper reversal and the presence of a relatively sharp contact between the ultramafic and mafic parts of the Layered Series, by *in situ* crystallization of a single input of phenocryst-poor parental magma. The model also explains the commonly developed, puzzling, phenomenon of the evolved nature of chilled margins compared with the bulk composition of sills, which is not easily explained by other models of magma evolution. Taken together these observations provide strong support for the proposed model and allow it to be used to explain the origin of other types of compositional profile observed in basic–ultrabasic sills.

The shape of the double-humped modal profile (Fig. 10) is defined from the base upward by rock sequences that compose four principal units: basal reversal, Layered Series, Upper Border Series and top reversal. Such subdivisions can be useful in understanding the origin of other types of compositional profiles. Figure 11 summarizes the different modal profiles observed in sills that can be interpreted as representing combinations of the four units. The obvious question is: Why are some units missing from these sill profiles? Does this reflect initial differences in parental magma composition or in conditions of magma evolution in the chamber? Finally, the most intriguing question: is it possible to produce all these profiles from the same magma composition given different conditions of magma evolution in the chamber?

There are several possible factors that are capable of determining the extent of development of various stratigraphic units in sills. Below I quantitatively examine the impact of two important parameters. The first is the initial temperature difference (ΔT), which is established in the liquid boundary layers after either remelting of the original chilled margins (Figs 12–14, a–d) or heating of cold country rock (Figs 12–14, e and f). The second is the initial magma composition. A relatively simple silica-undersaturated system *Ol–Pl–Cpx*, which is at the boundary between orthopyroxene- and nepheline-normative systems (Yoder & Tilley, 1962), is chosen for illustration of the basic principles. This system can be safely used to study the liquid line of descent of natural magma compositions with minor amounts of normative orthopyroxene (e.g. ore-bearing picrite–gabbrodolerite sills of the Noril'sk region, Czamanske *et al.*, 1995) or nepheline (e.g. alkaline sills of Skye, Simkin, 1967). Compositional profiles through the sills for three different parental magmas—super-cotectic X′ ($Ol + L$) (Fig. 12), cotectic Y ($Ol + Pl + L$) (Fig. 13) and eutectic E_1 ($Ol + Pl + Cpx + L$) (Fig. 14)—crystallizing at different values of ΔT, are successively considered. Special attention is paid to changes in the shape of the compositional profiles depending on the relative value of ΔT. The estimation of absolute values of ΔT cannot be carried out at present; those shown in Fig. 15 should be considered as highly approximate. Phase diagrams schematically showing the specific path of magma evolution supplement all figures. Compositional profiles (whole-rock mg-number, Cr, Ni) are accompanied by letter abbreviations, which mark topological elements of the phase diagram responsible for the origin of specific units of the sills. For simplicity, another essential factor that can affect the extent of development of various stratigraphic units in sills, namely, the size of the chamber, is ignored by considering the sills to be sheet-like bodies of constant thickness.

Compositional profiles of sills formed from parental magmas with super-cotectic compositions

Sills formed from parental magmas with super-cotectic compositions are widespread in nature. They exhibit the most pronounced modal and cryptic profiles. All the compositional profiles represented in Figs 9–11 actually belong to sills with super-cotectic magma compositions. Consequently, examination of this type of magma systems is of fundamental importance (Fig. 12).

(a) This is a case when ΔT is taken to be relatively small. In nature such a situation could occur when magma is injected into a hot, consolidating igneous massif or into country rocks heated by high-temperature regional metamorphism. Because the cooling effect of the country rocks is relatively small, the temperature contrast in the thermal boundary layers is not strong enough to generate effective Soret fractionation. In other words, there is no appreciable transfer of LMPC towards the chamber margins. As a result, neither basal nor roof compositional reversals are produced. Formation of the sill proceeds mainly by crystallization within a lower thermal boundary layer. Crystallization in the upper thermal boundary layer is almost completely suppressed as a result of vigorous thermal convection in the main magma body. The overall evolution of the magma is provided by the return of residual interstitial liquid from the crystallizing mush of the lower boundary layer to the interior of the magma body. The liquid follows a normal phase sequence $Ol + L$ (X′–Y, dunite) $\rightarrow Ol + Pl + L$ (Y–E_1, troctolite) $\rightarrow Ol + Pl + Cpx$ (E_1–E_3, olivine gabbro) as expected by classical fractional crystallization of initial liquid X′ lying in the primary field of olivine. The resulting sill is composed exclusively of a relatively thick Layered Series.

(b) This is a case when ΔT is sufficient to initiate Soret separation of magma at the lower thermal boundary layer with the subsequent formation of a basal compositional reversal. Vigorous thermal convection in the main magma body is still able to suppress Soret generation of a top reversal, but is unable to prevent the future crystallization of an Upper Border Series. The trend of crystallization in the basal reversal is exactly opposite that resulting from the position of parental magma X′ in the primary field of olivine: $Ol + Pl + Cpx$ (E_1, olivine gabbro) $\rightarrow Ol + Pl$ (E_1–Y, troctolite) $\rightarrow$ Ol (Y–X″, dunite). Upon reaching the lower crossover maximum, subsequent evolution of the magma will occur by the return of residual interstitial liquid from the crystallizing mush of the boundary layers to the interior of the magma body. At this time magma in the chamber will follow a normal fractionation trend $Ol + L$ (X″–Y, dunite) $\rightarrow Ol + Pl + L$ (Y–E_1, troctolite) $\rightarrow Ol + Pl + Cpx$ (E_1–E_3, olivine gabbro) resulting in the formation of the Layered and Upper Border Series.

(c) This is a case in which the magnitude of ΔT promotes more effective operation of Soret fractionation in the thermal boundary layers. This variant has already been discussed extensively above (Figs 9 and 10). Unlike case (b), vigorous thermal convection in the main body of magma is unable to prevent the generation of a top reversal. The thickness of the basal reversal is also substantially increased. As crystallization proceeds from the margins inwards, the parental magma passes through the upper and lower crossover maxima, giving rise to the formation of a compositional profile with a double-humped shape.

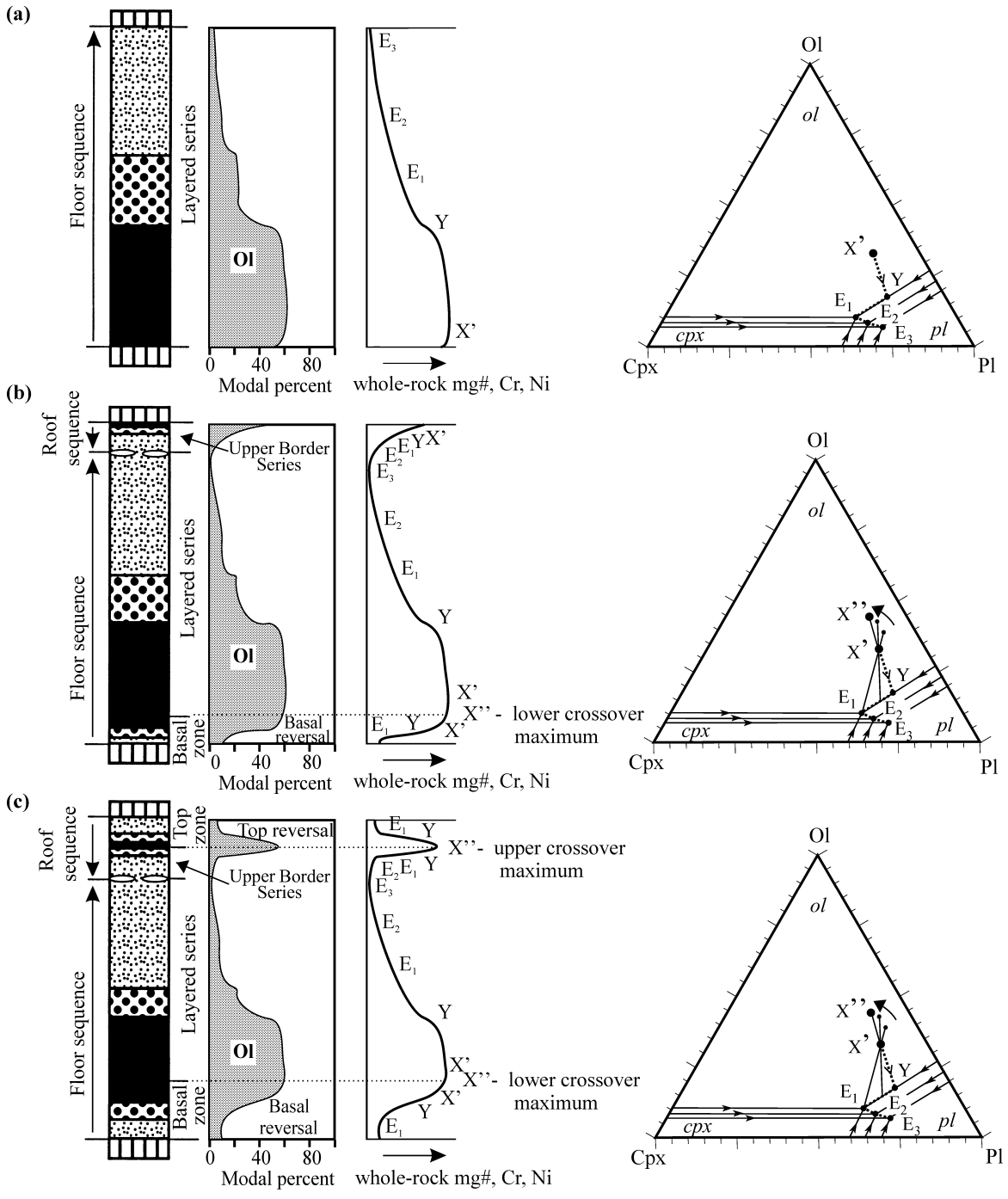

Fig. 12.

(d) This is a case in which ΔT is most favourable for the operation of Soret fractionation. Almost all of the main magma body takes part in supplying LMPC towards the chamber margins. In the most extreme case a sill forming under such conditions will predominantly be composed of two thick top and basal compositional reversals converging at the middle crossover maximum. The most primitive rock type, dunite, will occupy the middle part of the sill and there will be an overall gradual increase in whole-rock mg-number towards the centre of the sill.

(e) This is a case when heat flux from the convecting magma in the chamber cannot balance conductive heat flux into the country rock. In such a situation

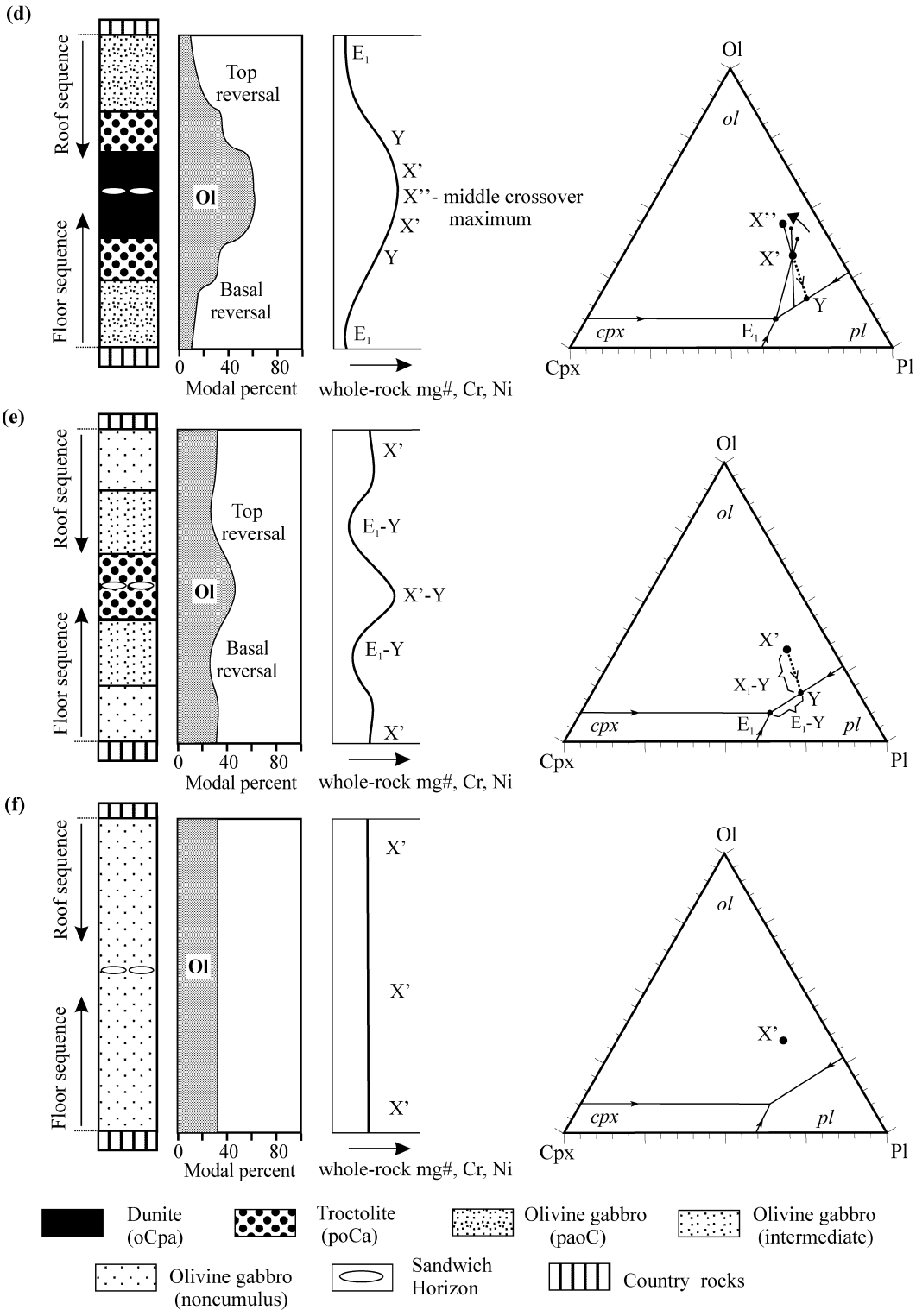

Fig. 12. (a)–(f) Diagrams illustrating the change in shape of the modal and cryptic profiles of sills formed from the same super-cotectic composition of the parental magma X′ under different degrees of temperature difference (ΔT) between country rocks and magma in the chamber. The relative magnitude of ΔT increases from (a) to (f) (see Fig. 15). The phase diagram of a silica-undersaturated system *Ol–Pl–Cpx* schematically shows specific paths of parental magma evolution for all cases. Letter abbreviations along the cryptic profiles (whole-rock mg-number, Cr, Ni) identify the topological elements of the phase diagram responsible for the origin of specific units of the sills. (See text for further discussion.)

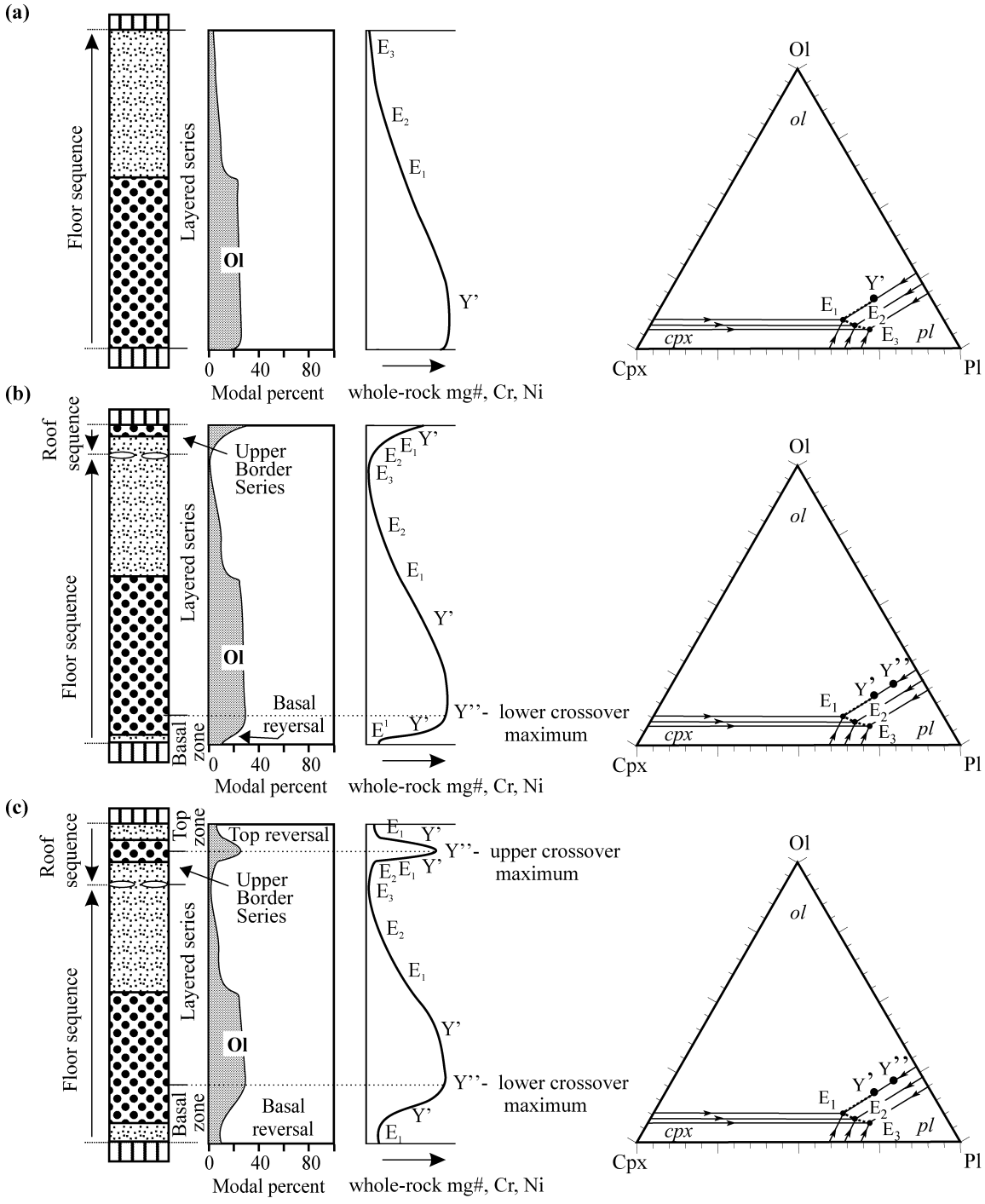

Fig. 13.

the ΔT becomes so high that rapid advance of the lower and upper thermal boundary layers is much higher than the velocity of transfer of LMPC towards the chamber margins. During this period, non-cumulus olivine gabbro, similar in composition to the parental magma X′, is formed. As solidification fronts move away from the margins the rate of their advance decreases and Soret fractionation starts to operate. The flux of LMPC towards the solidification fronts will not, however, be very effective and results in only slight differentiation of the remaining body of magma. This can eventually lead to the production of a central

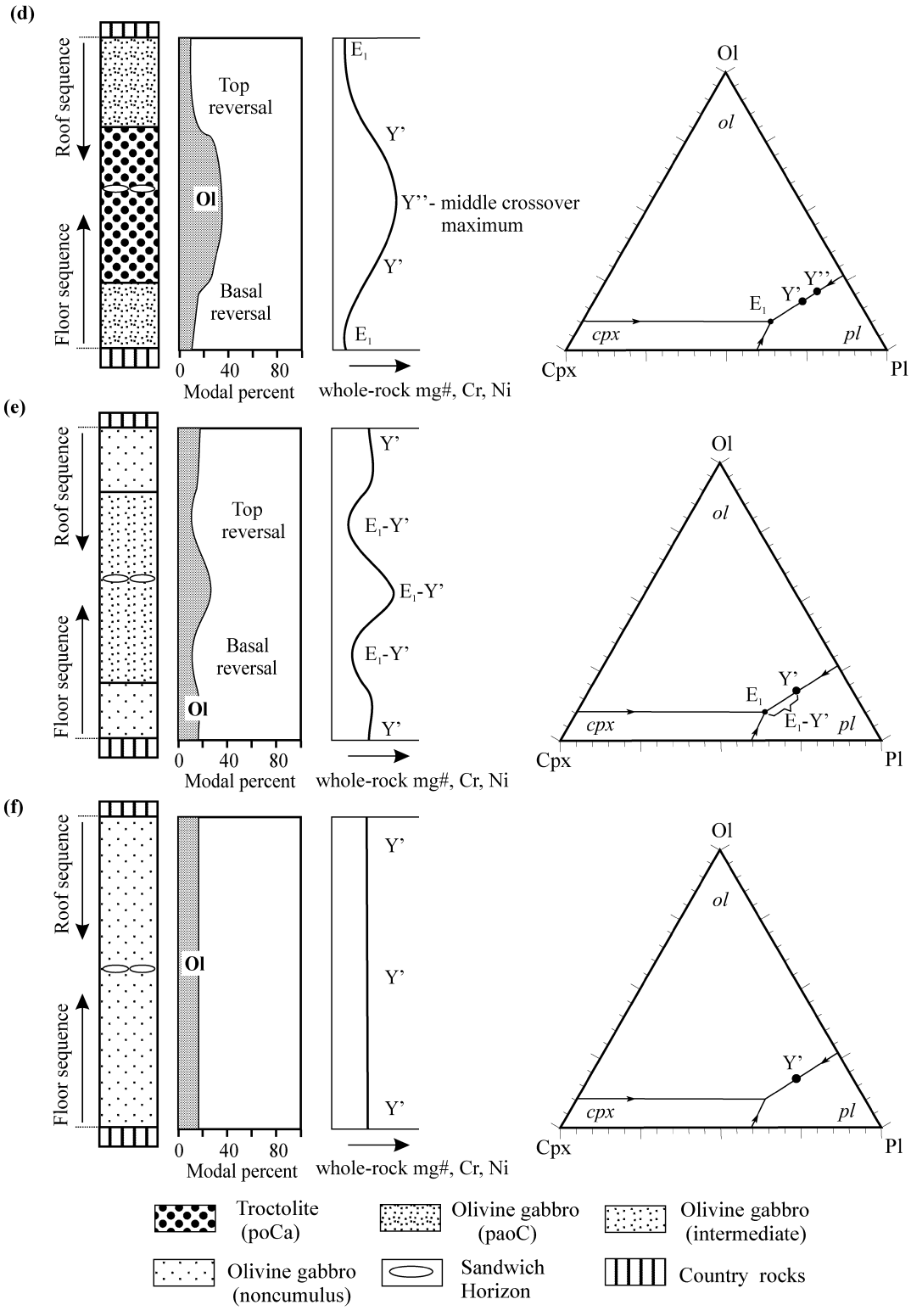

Fig. 13. (a)–(f) Diagrams illustrating the change in shape of modal and cryptic profiles of sills formed from the same cotectic composition of the parental magma Y′ under different degrees of temperature difference (ΔT) between country rocks and magma in the chamber. The relative magnitude of ΔT increases from (a) to (f) (see Fig. 15). The phase diagram of a silica-undersaturated system *Ol–Pl–Cpx* schematically shows specific paths of parental magma evolution for all cases. Letter abbreviations along the cryptic profiles (whole-rock mg-number, Cr, Ni) identify the topological elements of the phase diagram responsible for the origin of specific units of the sills. (See text for further discussion.)

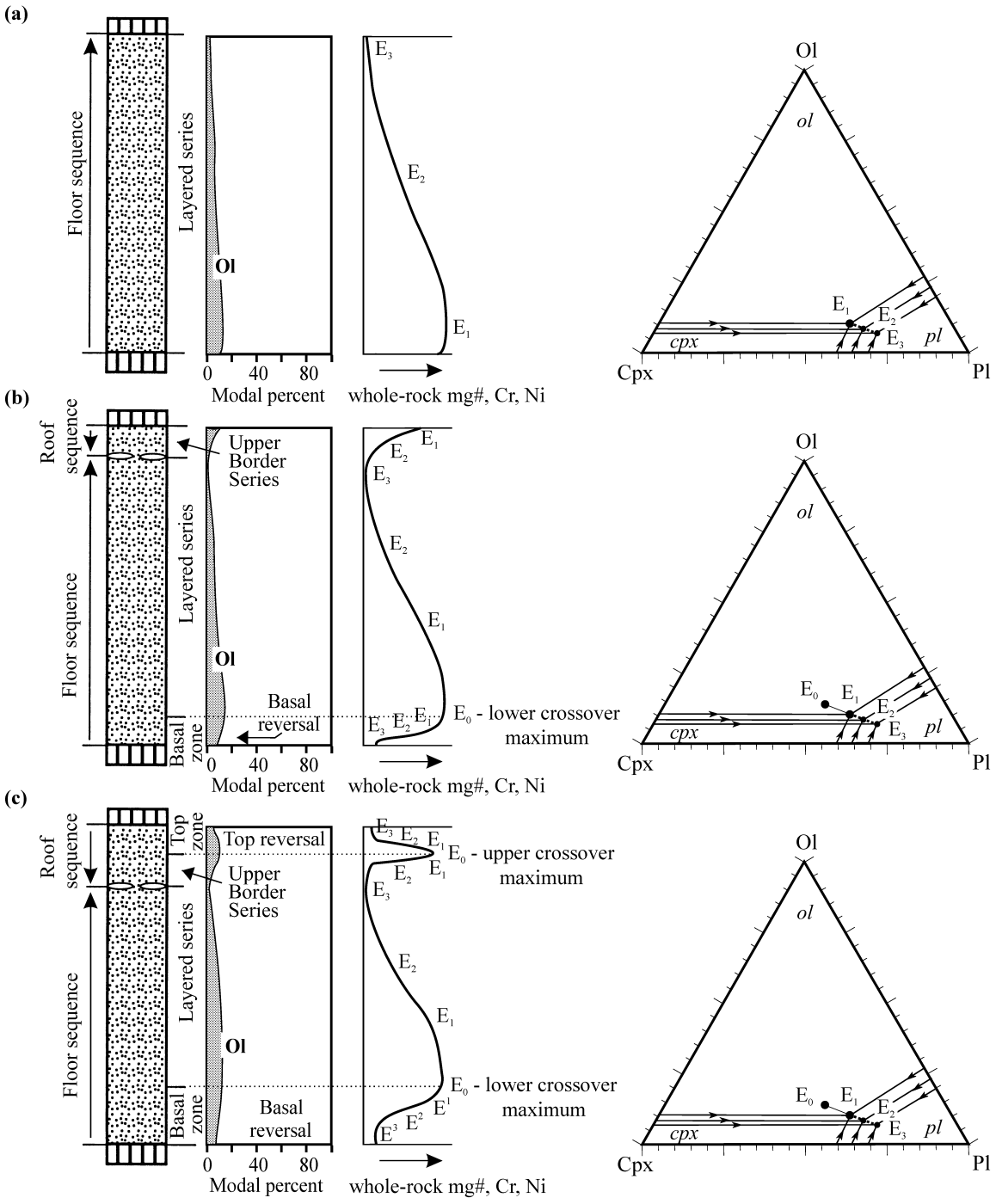

Fig. 14.

troctolite unit bordered by intermediate olivine gabbro containing a somewhat smaller amount of olivine than the adjacent non-cumulus olivine gabbro.

(f) In the last case, the imbalance between heat flux from the convecting magma in the chamber and conductive heat flux further increases. The very high ΔT produced makes any operation of Soret fractionation impossible for kinetic reasons. The whole body of magma crystallizes very rapidly with the formation of only one rock-type, a non-cumulus olivine gabbro, corresponding to the composition of the parental magma X′. Any evolution of the liquid is suppressed.

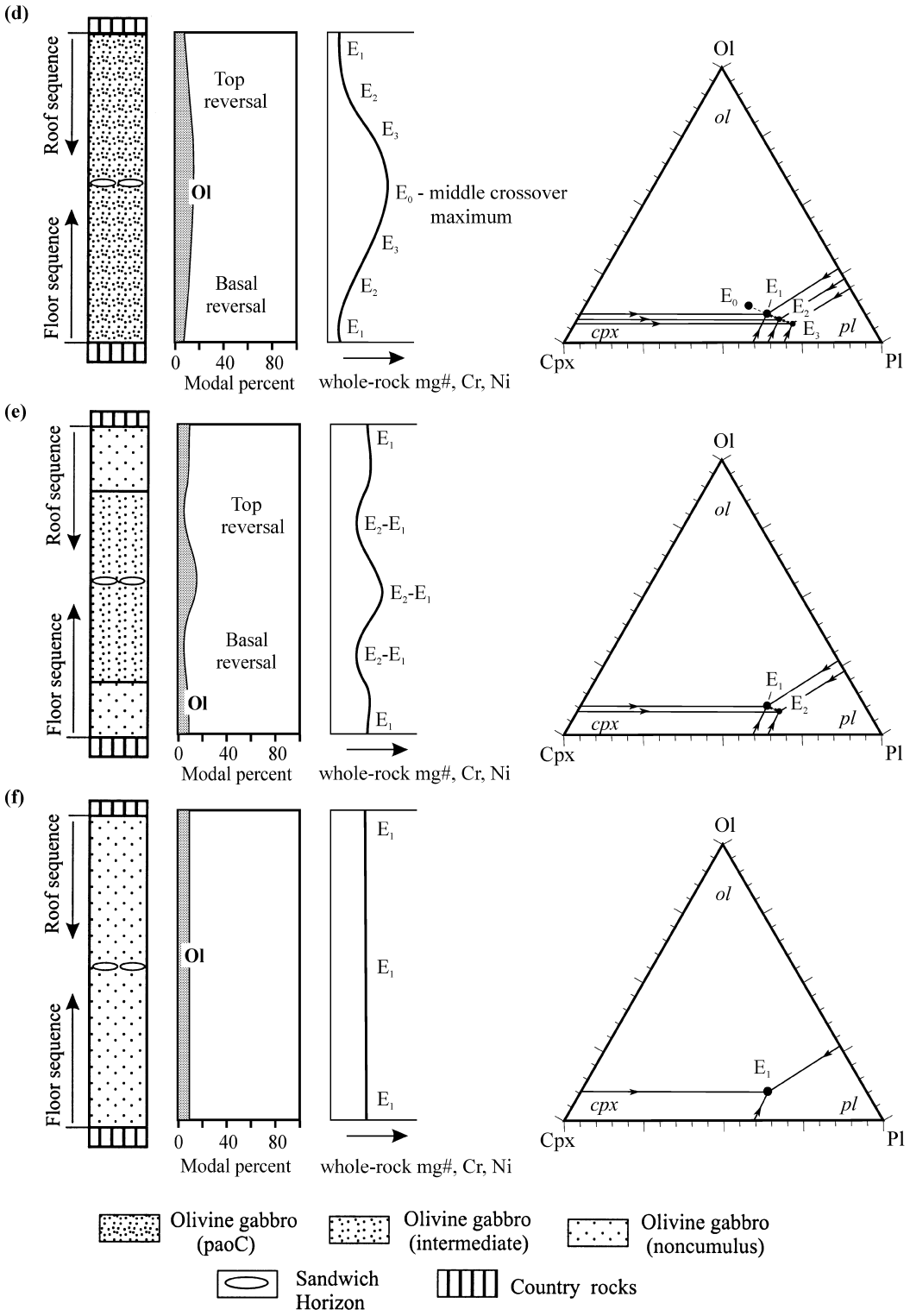

Fig. 14. (a)–(f) Diagrams illustrating the change in shape of modal and cryptic profiles of sills formed from the same eutectic composition of the parental magma E_1 under different degrees of temperature contrast between country rocks and magma in the chamber (ΔT). The relative magnitude of ΔT increases from (a) to (f) (see Fig. 15). The phase diagram of a silica-undersaturated system *Ol–Pl–Cpx* schematically shows specific paths of parental magma evolution for all cases considered. Letter abbreviations along the cryptic profiles (whole-rock mg-number, Cr, Ni) identify the topological elements of the phase diagram responsible for the origin of specific units of the sills. (See text for further discussion.)

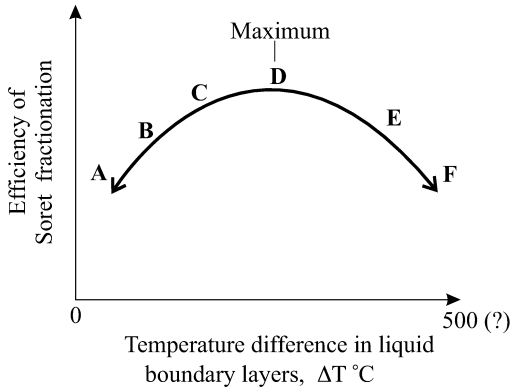

Fig. 15. Schematic diagram showing the relative efficiency of Soret fractionation as a function of the initial temperature difference (ΔT), which is established in the liquid boundary layers after remelting of the original chilled margins and/or heating of the cold country rock. The absolute values of ΔT are currently unknown; the shown estimation of absolute values of ΔT should be therefore considered as highly approximate.

The natural example of such an extreme case is a medium- to fine-grained thin sill showing no evidence of fractionation from the floor to the roof.

The scheme presented in Fig. 12 does not include two types of compositional profiles that consist of a combination of a Layered Series with an Upper Border Series (Fig. 11b) and with a basal reversal (Fig. 11e). The first type should probably be placed between the cases (a) and (b) (Fig. 12). The location of the second type in my scheme remains unclear. One explanation is that this type represents the type (b) or (c) (Fig. 12) where the upper rock sequences have been completely detached from the roof as a result of gravitational instability during the magmatic stage (Marsh, 1996).

Compositional profiles of sills formed from parental magma with cotectic and eutectic compositions

The nature of the processes leading to the formation of sills derived from parental magmas with cotectic (Y′) or eutectic (E_1) compositions are practically identical to those discussed above. The reason that I present Figs 13 and 14 is to demonstrate how the shape of modal profiles is progressively simplified as the parental magma approaches the eutectic composition. Super-cotectic sills are composed of three principal units—dunite, troctolite and olivine gabbro (Fig. 12)—whereas cotectic sills consist of troctolite and olivine gabbro units (Fig. 13) and eutectic sills are composed of only a single unit of olivine gabbro (Fig. 14). It is evident that in this succession the configuration of the modal profile approaches an I-shape. Nearly all of the eutectic sills from (a) to (f) (Fig. 14) are characterized by minor vertical variations in olivine abundance (in the range of 5–10%) and can therefore be roughly classified as I-shaped sills. On the other hand, the cryptic mineral and rock compositional profiles (whole-rock mg-number, Cr, Ni) within these sills (Fig. 14) can be fairly well developed and similar in all respects to those in the super-cotectic (Fig. 12) and cotectic sills (Fig. 13). For instance, the sill in Fig. 14b is cryptically S-shaped despite having an I-shaped modal distribution.

Some comments on the origin of various compositional profiles

As a whole, the tendency to develop basal and top reversals, which largely define the shape of the compositional profiles, depends on the variation in ΔT in the following manner (Figs 12–14). The reversals arise at the sill margins (b) and (c) and then progressively advance towards the centre of the body (d). After this, the direction of development of reversals changes to the opposite: they start to dampen out gradually from the chamber margins (e) and completely disappear in the middle of the body (f). Thus variant (d) represents a case of maximum development of both reversals (Fig. 15). Before case (d) the magnitude of ΔT is too small to provide a high efficiency of Soret fractionation; in contrast, after this case, ΔT is too great for Soret fractionation to occur effectively.

It is evident that with an increase in ΔT from (a) to (f), the extent of differentiation of the sills diminishes. In this process the thickness of the roof sequence increases and its lower boundary is displaced towards the centre of the chamber. In a similar manner the most primitive dunite unit also progressively shifts towards the centre of the sill, but upwards from the base of the body. A noteworthy consequence of this is that the composition of the 'Sandwich Horizon', i.e. the level at which the upper and lower solidification fronts converge, in cases (b) and (c) is the most evolved, whereas in cases (d) and (e) it represents the most primitive composition of the sills.

The variation in development of a basal chilled margin with increasing ΔT is also noteworthy. First, the composition of the chilled margin is consistent with the most primitive cumulate produced from the parental magma X′ [dunite, (a)], then with a product of crystallization of a eutectic point E_1 [olivine gabbro, (b)–(d)] followed by a chilled facies of parental magma X′ [noncumulus olivine gabbro, (e) and (f)]. It is obvious that only in the last two, rather rare, cases can the composition of chilled margins be taken as an indication of the parental magma composition.

It is also noteworthy that the shapes of the compositional profiles are very diverse and it is difficult to organize them into the three conventionally accepted

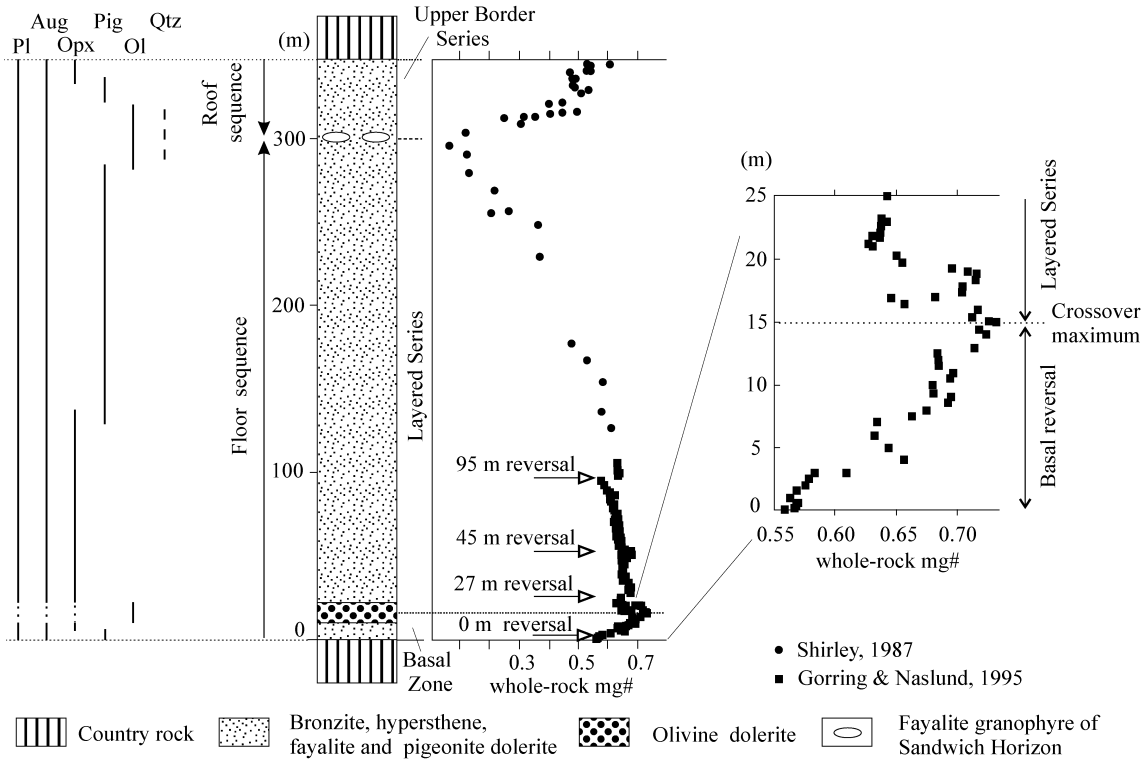

Fig. 16. Generalized stratigraphic section through the Palisades sill (New Jersey, USA) showing the development of cumulus (continuous lines) and intercumulus (dashed lines) minerals and variations in whole-rock mg-number with stratigraphic height. The figure is based mainly on Walker *et al*. (1973), Shirley (1987) and Gorring & Naslund (1995). The Basal Zone of the sill represents a well-developed compositional reversal characterized by an inverse order of phase crystallization $Pig + Pl + Aug \rightarrow Pig + Opx + Pl + Aug \rightarrow Opx + Pl + Aug \rightarrow Opx + Pl\,(?) \rightarrow Opx\,(?) \rightarrow Ol$ and a bottom mg-number enrichment trend. The crossover maximum lies ~15 m above the basal contact. Apart from the basal reversal minor geochemical reversals at 27, 45 and 95 m are also indicated.

S-, D-, and I-types. However, variant (b) can be classified as S-shaped, variant (d) is reminiscent of a D-shaped profile and variant (f) is most similar to an I-shaped profile (Figs 12 and 13). Further limitation of the use of the conventional classification of natural sills based on profile shape comes from the apparent discrepancy between the shapes of modal and cryptic profiles in sills that crystallized from parental magma with a eutectic composition (Fig. 14). The main inference that can be drawn from the diagrams presented in Figs 12–14 and the above discussion is that, under favourable conditions, various types of compositional profiles can be produced from the same parental magma. Which type of modal and cryptic profile will be produced is primarily dependent on the initial temperature difference (ΔT), which is established in the liquid boundary layers after remelting of original chilled margins and/or heating of cold country rock (Fig. 15). The shape of the modal profile is also strongly dependent on the composition of the initial parental magma. Even with the most favourable value of ΔT it is impossible to produce the well-developed modal profiles if the initial parental magma is close to a eutectic composition. The only possible modal profile that can be produced from a eutectic composition is I-shaped, although the shapes of cryptic profiles can vary.

PALISADES SILL: AN ORIGIN FROM A SINGLE PULSE OF MAGMA?

The proposed *in situ* crystallization model can be used to provide constraints on the origin of the olivine zone (OZ) at the bottom of the Palisades sill, New Jersey, USA. The 350 m thick Palisades sill is cited in many igneous petrology texts as the classic example of a vertically differentiated sill with well-developed floor and roof sequences meeting at the Sandwich Horizon (Fig. 16). The floor sequence is ~7 times thicker than the roof sequence. The sill displays a well-developed differentiation trend from olivine dolerite through bronzite, hypersthene and pigeonite dolerites to fayalite dolerite and granophyre (Walker *et al*., 1973). Ignoring the minor cumulus phases such as apatite, biotite and zircon, the crystallization sequence in the

Layered Series can be defined as follows: $Ol \rightarrow Opx$ (?) $\rightarrow$ $Opx + Pl$ (?) $\rightarrow$ $Opx + Pl + Aug \rightarrow Pig + Opx + Pl + Aug \rightarrow Pig + Pl + Aug \rightarrow Ol + Pl + Aug + Qtz$. The crystallization sequence in the Upper Border Series differs from that of the Layered Series only by its lack of olivine dolerite. The Palisades sill is commonly considered to have been formed by multiple magma injections because of four geochemical reversals in the normal tholeiitic differentiation trend observed at 95, 45, 27 and 0 m above the basal contact (Shirley, 1987; Gorring & Naslund, 1995). There are, however, good grounds to believe that interpretation of these geochemical reversals does not necessarily require multiple magma injections. In particular, it has been recently shown that the sharp reversal at 95 m is caused by repetition of the stratigraphic section as a result of normal faulting at this level (Gorring & Naslund, 1995). Formation of minor geochemical reversals at 45 and 27 m can be principally attributed to a sudden change in an intensive parameter such as pressure or water fugacity (Shirley, 1987, p. 840) although magma recharge events cannot be completely ruled out. The reversal starting from the basal contact and comprising the well-known OZ is commonly accepted (Gorring & Naslund, 1995) as the major evidence for magma recharge into the chamber and therefore deserves detailed consideration.

The first investigators of the Palisades sill (Lewis, 1908; Walker, 1940) believed that the OZ originated by gravity settling of early-formed olivine crystals within a quartz-normative magma injected as a single pulse. All subsequent investigators of the sill started from the assumption that the OZ is a kind of anomaly that owes its existence to the operation of some external factors. In particular, Walker (1969), despite reconfirming that the OZ is a result of gravity settling of olivine, attributed the OZ to a second major magmatic injection into the chamber. Shirley (1987) and Husch (1990) also interpreted the OZ as a second olivine-normative magma injection; however, they dismissed gravity settling in their models on physical and petrological grounds. In contrast, Steiner *et al.* (1992) concluded that the OZ is a product of neither *in situ* gravity settling nor externally derived multiple magma injections. They proposed a Cumulus–Transport–Deposition model in which the OZ was considered as an early accumulation of olivine, owing its existence to the internal processes of crystal settling and sedimentation. Gorring & Naslund (1995) returned to the idea of a second injection of magma, suggesting that the OZ resulted from the emplacement of a heterogeneous olivine phenocryst-bearing magma from a compositionally stratified storage chamber. It seems that the combination of nearly all the processes of magma differentiation (magma-chamber recharge, flow differentiation, gravity settling, two-phase convection, and crystal sorting processes), except *in situ* crystallization, have already been involved in the explanation of the origin of the OZ. I intend to show here that the OZ of the Palisades sill is not an anomaly but rather a common consequence of *in situ* crystallization of parental magma undergoing Soret fractionation.

Analysis of the available data shows that the lower section of the Palisades sill possesses all the features of a typical basal reversal. It is characterized by: (1) a bottom mg-number enrichment trend (Fig. 16); (2) a lack of local mass balance between bulk composition of the intrusion and the chilled margin (Husch, 1990); (3) order of phase crystallization $Pig + Pl + Aug \rightarrow Pig + Opx + Pl + Aug \rightarrow Opx + Pl + Aug \rightarrow Opx + Pl$ (?) $\rightarrow$ Opx (?) $\rightarrow$ Ol that is inverse to that observed in the lower part of the Layered Series (Walker *et al.*, 1973; Fig. 16). As outlined above, the origin of such a basal reversal can be adequately modelled by *in situ* crystallization of a range of liquids successively produced by Soret fractionation from a parental magma and spanning in reverse sequence its entire liquid line of descent. The central point here is how the OZ could be produced from a parental quartz-normative magma, as implied by the bulk composition of the sill, which lies in the primary field of orthopyroxene (Fig. 17). My explanation is that removal of LMPC from this magma as a result of relatively high efficiency of Soret fractionation eventually shifts magma in the chamber into the olivine primary field (crossover maximum M1). It is important to note, however, that if Soret fractionation is less effective, the magma in the chamber can remain within the primary field of orthopyroxene (crossover maximum M2). As a result the OZ will not form. Thus local variations in the effectiveness of Soret fractionation can explain why the OZ does not extend as a prominent feature along the whole Palisades sill and in places disappears completely (Walker, 1969).

In more detail the trend of liquid evolution via Soret fractionation is shown in volume phase equilibria diagrams depicting changes in liquidus relationships with increase in mg-number of liquids produced by Soret fractionation from a parental magma of the Palisades sill (Fig. 18). With a decrease in a temperature contrast the liquids crystallizing in lowermost regions of the thermal boundary layers gradually change their composition from the $Pl + Aug + Pig + L$ cotectic (1 in Fig. 18a) towards the $Ol + L$ primary volume (M1 in Fig. 18d). This is accompanied by a gradual contraction of the primary volume of pigeonite within the phase diagrams as a consequence of a progressive increase in mg-number of these liquids. The changes in mineral assemblages observed in the basal reversal of the Palisades sill can be explained as follows.

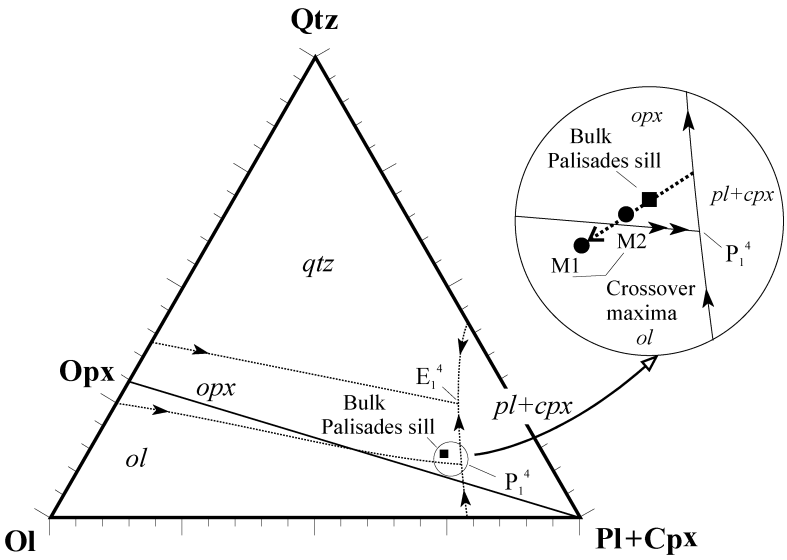

Fig. 17. A projection plane of the isobaro-isoplethic section *Ol–Cpx–Pl–Qtz* showing that the parental quartz-normative magma of the Palisades sill, as implied by its bulk composition, lies in the primary field of orthopyroxene. An enlarged portion of the diagram aims to illustrate that the development of the olivine zone (OZ) as part of the basal reversal is greatly dependent on the effectiveness of Soret fractionation. Substantial removal of LMPC from this magma as a result of relatively high efficiency of Soret fractionation eventually shifts magma in the chamber into an olivine primary field (crossover maximum M1) providing the formation of the OZ. If Soret fractionation is less effective, the magma in the chamber can remain within the primary field of orthopyroxene (crossover maximum M2). As a result, formation of the OZ will become impossible. Bulk composition of the Palisades sill is from Shirley (1987). Phase relations along the projection plane are consistent with melt parameters mg-number = 50–75, An = 60–70 and $P < 1$ kbar [slightly modified from Dubrovskii (1998)]. Compositions of the components are expressed in wt %. E_1^4, $Qtz + Opx + Cpx + Pl = L$; P_1^4, $Opx + Cpx + Pl = L + Ol$.

At the lowest mg-number value (Fig. 18a) the Soret-produced liquid 1 lying on the $Pl + Aug + Pig + L$ cotectic crystallizes the lowermost dolerite consisting of the opx-free mineral assemblage pab#C. Here orthopyroxene is absent from the assemblage, as its primary volume is separated from that of augite by the pigeonite primary volume. The overlying dolerite pabb#C forms from the more primitive Soret-produced liquid 2 as it crystallizes along a path $Pl + Aug + Pig + Opx + L$ reaction curve $\rightarrow Pl + Aug + Pig + L$ cotectic. The formation of this assemblage comprising three coexisting pyroxenes with plagioclase has been made possible owing to the shrinking of the pigeonite volume caused by increase in melt mg-number (Fig. 18b). With further increase in mg-number and related contraction of the pigeonite volume (Fig. 18c) the formation of pigeonite-bearing assemblage becomes, however, impossible because of disappearance of a contact surface between the primary volumes of plagioclase and pigeonite. Therefore the Soret-produced liquid 3 crystallizing along a path $Pl + Opx + L$ cotectic surface $\rightarrow$ $Pl + Opx + Aug + L$ cotectic gives way to dolerite with the pig-free assemblage pabC.

Progressive removal of LMPC from the parental magma of the Palisades sill finally shifts magma in the chamber from the primary volume of orthopyroxene into that of olivine (crossover maximum M1 in Figs 17 and 18d). The crystallization of the liquid M1 results in formation of olivine-bearing dolerite oCpba along a path $Ol + L$ volume $\rightarrow Ol + Opx + L$ reaction surface $\rightarrow Opx + L$ volume $\rightarrow Pl + Opx + L$ surface $\rightarrow Pl + Opx + Aug + L$ cotectic. The resulting basal reversal produced from the Soret-produced liquids 1–M1 will comprise, from the base upwards, a sequence of dolerites with the following mineral composition: pab#C, pabb#C, pabC, pbCa (?), bCpa (?), oCpba. It should be noted that phase diagrams suggest that transition from dolerite pabC to overlying dolerite oCpba should occur through dolerite of intermediate composition (pbCa and bCpa) that has not been yet reported for the Palisades sill. I suppose that this is probably related to difficulties in petrographic identification of cumulus and intercumulus phases, as up to 40–50% of the volume of the dolerites is produced from crystallization of trapped intercumulus liquid (Shirley, 1987). It would be therefore rather difficult to find petrographic evidence for liquid fractionation, for example, along an $Ol + Opx + L$ reaction surface or through an $Opx + L$ volume despite the fact that phase equilibria topology almost certainly suggests this must have happened to produce the olivine dolerite.

Thus all four geochemical reversals identified within the lower 100 m of the Palisades sill can, in principle, be explained without involving multiple magma

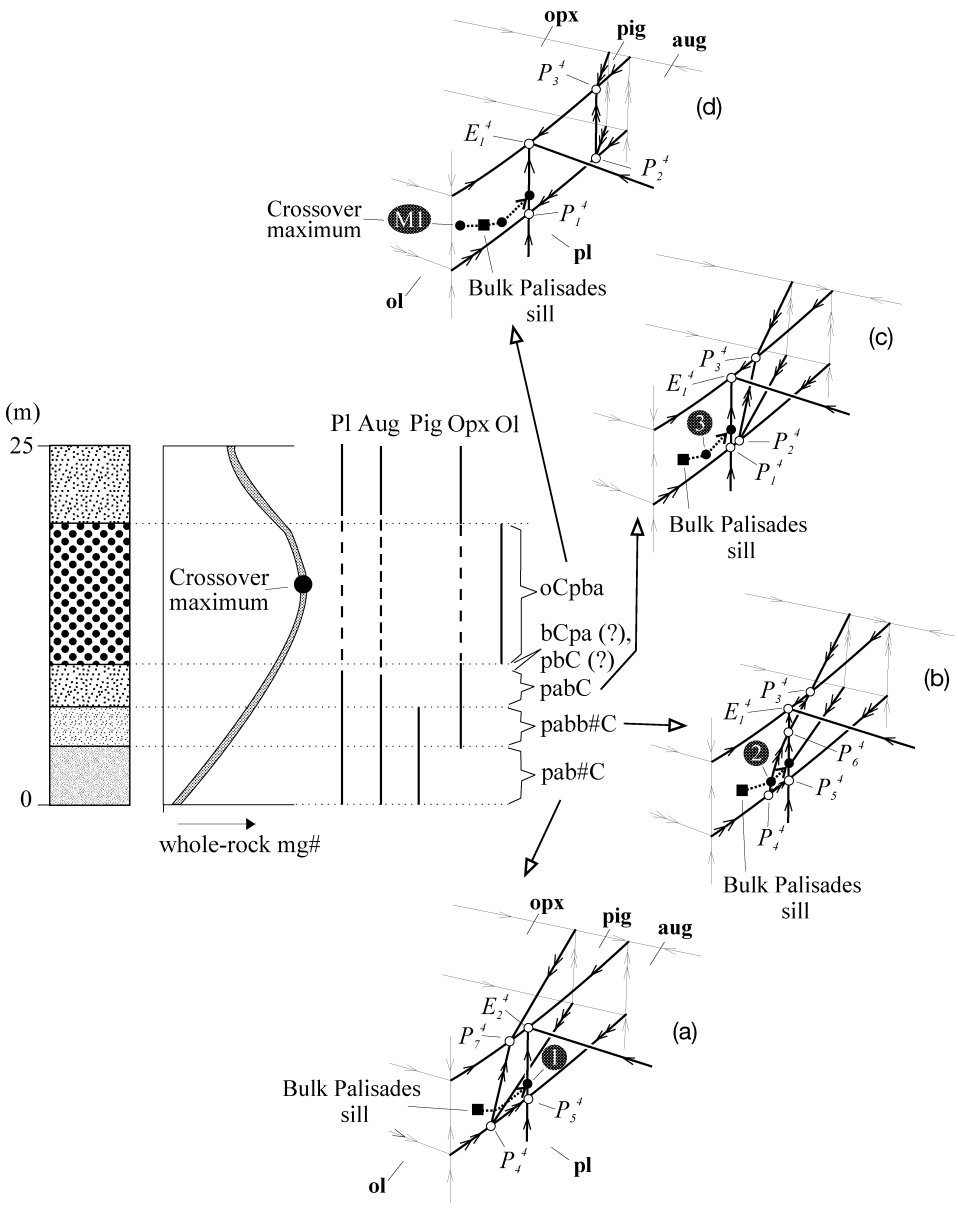

Fig. 18. Schematic stratigraphic section through the basal reversal of the Palisades sill (New Jersey, USA) showing the development of cumulus (continuous lines) and intercumulus (dashed lines) minerals and a general trend in whole-rock mg-number with height. Formation of each cumulus type of dolerite (pab#C, pabb#C, pabC, pbCa (?), bCpa (?) and oCpba) is shown on isobaric–isoplethic sections Ol^{25-50}–*Aug*–Pl^{60}–*Qtz* that systematically change in topology as a result of an increase in the mg-number of the melt [simplified from Latypov *et al.* (2001)]. The phase diagrams represent liquidus phase relations in the interior of the tetrahedron *Ol–Cpx–Pl–Qtz* at atmospheric pressure. Bold continuous curves indicate liquidus lines within a tetrahedron. Fine lines in the front and back of each diagram are located on the *Ol–Pl–Qtz* and *Ol–Aug–Qtz* faces of a tetrahedron, respectively. Invariant points in the interior of the tetrahedron are shown as open circles. Cotectic and reaction lines are indicated by single- and double-headed arrows, respectively. Reactions and phase assemblages in invariant points are listed in Table 4. Arrows point toward falling temperature. The filled circles 1, 2, 3 and M1 indicate a gradual shift of crystallizing stagnant lowermost regions of liquid boundary layers from *Pl* + *Aug* + *Pig* + *L* cotectic towards an olivine primary volume with decrease in the temperature difference of boundary layers. Cumulate abbreviations as in Fig. 3. (See text for further explanation.)

injections. It is therefore not inconceivable that future deeper insight into the sill's origin will establish that it could crystallize as a closed system from a single pulse of magma.

CONCLUSIONS

Adequate explanation for the nature of different compositional profiles in sills can be provided by a model of *in situ* crystallization (e.g. Jaupart & Tait, 1995; Tait &

Table 4: Reactions and phase assemblages illustrated in Fig. 18

Notation	Phase equilibria
E_1^4	Qtz + Opx + Aug + Pl = L
E_2^4	Qtz + Pig + Aug + Pl = L
P_1^4	Opx + Aug + Pl = L + Ol
P_2^4	Opx + Aug = L + Ol + Pig
P_3^4	Qtz + Opx + Aug = L + Pig
P_4^4	Pig + Pl = L + Ol + Opx
P_5^4	Pig + Aug + Pl = L + Ol
P_6^4	Opx + Aug = L + Pig + Pl
P_7^4	Qtz + Pig + Pl = L + Opx

Jaupart, 1996) in combination with the Soret fractionation mechanism for the origin of basal and top reversals (Latypov, 2003). It is proposed that the formation of basal and top reversals takes place through liquid boundary layers maintained out of equilibrium as a result of a temperature gradient imposed by the cold country rock. In contrast, the Layered and Upper Border Series originate predominantly through the crystal–liquid boundary layers developing in conditions of equilibrium. The key factors for the formation of compositional profiles are (1) the initial temperature difference (ΔT), which is established in the liquid boundary layers after remelting of the original chilled margins and/or heating of the cold country rock, and (2) the initial parental magma composition that can vary from super-cotectic through cotectic to near-eutectic. The temperature difference, controlling the efficiency of development of the basal and top reversals, is responsible for the formation of both modal and cryptic profiles. Various modal and cryptic profiles can be produced by *in situ* crystallization, even from the same phenocryst-poor parental magma, depending on variations in ΔT. D-shaped profiles originate from crystallization of the parental magmas under conditions of maximum efficiency in the development of both basal and top compositional reversals (intermediate value of ΔT). The most common S-shaped and double-humped profiles reflect sill formation from parental magmas under conditions of moderate efficiency in the development of basal and top reversals (relatively low value of ΔT). I-shaped profiles can result from very rapid crystallization of the parental magma, preventing the formation of compositional reversals and any liquid evolution in the chamber (relatively high value of ΔT).

The initial parental magma composition has a major impact on the shape of the modal profiles. The most favourable parental magmas for the formation of sills with S-, double-humped and D-shaped modal profiles are of super-cotectic and, to a lesser degree, of cotectic composition. Sills forming from parental magmas with near-eutectic compositions will always develop roughly I-shaped modal profiles, but can display all known shapes of cryptic profiles depending on variations in ΔT. The advantage of the proposed mechanism is that it does not appeal to any external or accidental processes such as multiple magma emplacement, the initial amount of phenocrysts and their mode of distribution in the injected magma, or the ability of newly formed crystals to settle, etc. All that is necessary to produce a specific shape of compositional profile is an appropriate temperature gradient imposed by the cold country rocks on the liquid boundary layers of a phenocryst-poor parental magma of a certain composition. Other mechanisms of magma evolution, such as crystal settling, flow differentiation or multiple magma injections, will probably also play some role in the generation of the resulting compositional profile, but their contribution is generally relatively small.

The most important consequences and inferences of the proposed model relevant for the formation of basic–ultrabasic sills are as follows:

(1) a sill is principally composed of floor and roof sequences that meet at the level of the Sandwich Horizon. The floor sequence of the sill comprises the Basal Zone and the Layered Series, whereas the roof sequence contains the Top Zone and Upper Border Series. The lines of demarcation between the coupled units of the floor and roof sequences run through the lower and upper crossover maxima exhibiting the most primitive mineral and rock compositions in the entire section of the sill. The Basal and Top Zones, being mirror images of the Layered and Upper Border Series sequences, respectively, are therefore referred to as basal and top reversals.

(2) The mirror image of basal and top reversals results from the operation of non-equilibrium Soret fractionation, which works in a manner distinctly opposite to that of equilibrium crystal–liquid fractionation, which produces the Layered and Upper Border Series.

(3) Well-developed basal reversals can be used to obtain a rough estimate of the parental magma composition and reconstruction of its phase crystallization sequence; taking the chilled margins of intrusions as representative of the parental magma composition can lead to misleading results because the original chilled margins do not commonly survive, as a result of intensive remelting; the compositions of the secondary chilled margins are generally compatible with the

most evolved cotectic assemblages of the parental magma line of descent.

(4) Olivine-rich basal and roof picritic units of S-shaped sills are the result of *in situ* crystallization of the same pulse of parental magma whose composition lies within the primary volume of olivine.

(5) The commonly observed sharp transition from picritic to gabbroic units marked by an abrupt decrease in olivine content is related to a shift of the crystallizing magma from the $Ol + L$ field to the $Ol + Pl + L$ cotectic; the subsequent decrease in olivine content in gabbroic units is attributed to the decrease of olivine proportions upon reaching the $Ol + Pl + Cpx + L$ eutectic point.

(6) The mineral compositions (e.g. Fo % in olivine) that can be reliably used for estimation of the parental magma composition occur slightly above and below the level of the lower and upper crossover maxima marking the upper and lower limits of the basal and top reversals, respectively.

This study clearly shows that liquidus phase diagrams are of great importance for understanding the processes responsible for the crystallization of igneous intrusions. This conclusion is far from novel but it is worth emphasizing. By way of illustration, one can mention the 'puzzling' phenomenon of the abrupt drop in olivine content at the boundary between picritic and troctolitic–gabbroic units in sills. It is surprising that this obvious consequence of a shift from the olivine primary field to the plagioclase–olivine cotectic is often cited as firm evidence for the formation of these units from two pulses of magma of contrasting composition. In this context it is not unlikely that our common appeal to some external forces such as multiple magma injections, to explain various 'anomalous' features or discontinuities observed in sills, is simply an indication of our inadequate understanding of the dynamics of differentiation of the multi-component natural melts. The origin of one such 'anomalous' feature, namely, occurrence of the complex isotopic profiles in some S-shaped and double-humped sills which cannot be attributed to contamination of the magma by local country rocks (e.g. Czamanske *et al.*, 1994; Foland *et al.*, 2000), will be discussed in a separate paper.

ACKNOWLEDGEMENTS

The original stimulus for this work stems from interesting discussions on the origin of well-known ore-bearing Noril'sk intrusions with V. A. Fedorenko and G. K. Czamanske. I am particularly indebted to M. I. Dubrovskii, A. A. Ariskin, B. D. Marsh, A. R. McBirney, D. Walker, E. V. Sharkov and E. G. Konnikov for a very thorough reading of an early draft of the manuscript and many constructive comments and much good advice, not all of which I could heed. I wish to express special thanks to Richard Wilson and F. G. F. Gibb for many helpful suggestions and thoughtful comments that helped to improve the manuscript. The paper essentially benefited from discussions of its various aspects with T. T. Alapieti and S. Tait. I am indebted to M. Wilson, M. O'Hara, I. H. Campbell and F. J. Spera for their helpful comments and suggestions, which greatly contributed to improving the manuscript. I am also grateful to R. Wilson and Stacy Saari for editing that led to a significant improvement in the wording of the early versions of the text. The research was supported by grants from the Thule Institute of the University of Oulu, the Center for International Mobility (Helsinki, Finland), E. J. Sariolan Foundation (Helsinki, Finland), Tauno Tönningiin Foundation (Oulu, Finland), Academy of Finland (Project N51005 and N203456), and the RFBR-France (Project N01-05-22001). This paper is dedicated to the memory of Nikolay Leonidovich Balabonin.

REFERENCES

Alapieti, T. T. (1982). *The Koillismaa Layered Igneous Complex, Finland—its Structure, Mineralogy and Geochemistry, with Emphasis on the Distribution of Chromium. Geological Survey of Finland, Bulletin* **319**, 116 pp.

Ariskin, A. A. (1999). Phase equilibria modelling in igneous petrology: use of COMAGMAT model for simulating fractionation of ferro-basaltic magmas and genesis of high-alumina basalt. *Journal of Volcanology and Geochemical Research* **90**, 115–162.

Ariskin, A. A. & Barmina, G. S. (2000). *Modelling of Phase Equilibria upon Crystallization of Basalt Magmas*. Moscow: Nauka, MAIK 'Nauka/Interperiodica', 363 pp. (in Russian).

Baker, M. B. & Grove, T. L. (1985). Kinetic control on pyroxene nucleation and metastable liquid lines of descent in basaltic andesite. *American Mineralogist* **70**, 279–287.

Bédard, J. H. J. (1987). The development of compositional and textural layering in Archaean komatiites and in Proterozoic komatiitic basalts from Cape Smith, Quebec, Canada. In: Parson, I. (ed.) *Origin of Igneous Layering*. Dordrecht: D. Reidel, pp. 399–418.

Bowen, N. L. (1915). The crystallization of haplobasaltic, haplodioritic and related magmas. *American Journal of Science* **236**, 161–185.

Campbell, I. H. (1978). Some problems with the cumulus theory. *Lithos* **11**, 311–323.

Cawthorn, R. G. & McCarthy, T. S. (1980). Variations of magnetite from the upper zone of the Bushveld complex—evidence for heterogeneity and convection currents in magma chambers. *Earth and Planetary Science Letters* **46**, 335–343.

Cawthorn, R. G. & McCarthy, T. S. (1985). Incompatible trace element behavior in the Bushveld Complex. *Economic Geology* **46**, 335–343.

Chalokwu, C. I., Grant, N. K., Ariskin, A. A. & Barmina, G. S. (1993). Simulation of primary phase relations and mineral

compositions in the Partridge River intrusion, Duluth Complex, Minnesota: implications for the parent magma composition. *Contributions to Mineralogy and Petrology* **114**, 539–549.

Czamanske, G. K., Wooden, J. L., Zientek, M. L., Fedorenko, V. A., Zen'ko, T. E., Kent, J., King, B.-S. W., Knight, R. J. & Siems, D. F. (1994). Geochemical and isotopic constraints on the petrogenesis of the Noril'sk–Talnakh ore-forming system. *Proceedings of the Sudbury–Noril'sk Symposium. Ontario Geological Survey Special Publication* **5**, 313–342.

Czamanske, G. K., Zen'ko, T. E., Fedorenko, V. A., Calk, L. C., Budahn, J. R., Bullock, J. H., Jr, Fries, T. L., King, B.-S. W. & Siems, D. F. (1995). Petrographic and geochemical characterization of ore-bearing intrusions of the Noril'sk type, Siberia; with discussion of their origin. *Resource Geology Special Issue* **18**, 1–48.

Distler, V. V., Smirnov, A. V., Grokhovskaya, T. L., Philimonova, A. A. & Muravizkaya, G. N. (1979). The stratification, cryptic variation and the formation of the sulphide mineralization of the differentiated trap intrusions. In: Smirnov, V. I. (ed.) *The Formation of Magmatic Ore Deposits*. Moskow: Nauka, pp. 211–269 (in Russian).

Donaldson, C. H. (1976). An experimental investigation of olivine morphology. *Contributions to Mineralogy and Petrology* **57**, 187–213.

Donaldson, C. H., Usselman, T. M., Williams, R. J. & Lofgren, G. E. (1975). Experimental modelling of the cooling history of Apollo 12 olivine basalts. *Proceedings of the 6th Lunar Science Conference. Geochimica et Cosmochimica Acta Supplement* 843–869.

Dowty, E. (1980). Crystal growth and nucleation theory and the numerical simulation of igneous crystallization. In: Hargraves, R. B. (ed.) *Physics of Magmatic Processes*. Princeton, NJ: Princeton University Press, pp. 419–485.

Drever, H. I. & Johnston, R. (1957). Crystal growth of forsteritic olivine in magmas and melts. *Transactions of the Royal Society of Edinburgh* **63**, 289–315.

Drever, H. I. & Johnston, R. (1958). The petrology of picritic rocks in minor intrusions—a Hebridean group. *Transactions of the Royal Society of Edinburgh* **63**, 459–499.

Drever, H. I. & Johnston, R. (1967) The ultrabasic facies in some sills and sheets. In: Wyllie, P. J. (ed.) *Ultramafic and Related Rocks*. New York: Wiley, pp. 51–63.

Dubrovskii, M. I. (1998). *Differentiation Trends of the Standard Alkalinity Olivine-normative Magmas and Corresponding Rock Series*. Apatity: Kola Science Center, 336 pp. (in Russian).

Duzhikov, O. A. & Distler, V. V. (1992) *Geology and Metallogeny of Sulfide Deposits, Noril'sk Region, USSR. Society of Economic Geologists, Special Publication* **1**, 242 pp.

Eales, H. V. & Cawthorn, R. G. (1996). The Bushveld Complex. 181–229. In: Cawthorn, R. G. (ed.) *Layered Intrusions. Developments in Petrology 15*. Amsterdam: Elsevier, pp. 181–229.

Faithfull, J. W. (1985). The Lower Eastern Layered Series of Rum. *Geological Magazine* **122**, 459–468.

Flett, J. S. (1931). The Blackness teschenite. *Summary of Progress of Geological Survey of Great Britain* **3**, 39–45.

Foland, K. A., Gibb, F. G. F. & Henderson, C. M. B. (2000). Pattern of Nd and Sr isotopic ratios produced by magmatic and postmagmatic processes in the Shiant Isles Main Sill, Scotland. *Contributions to Mineralogy and Petrology* **139**, 655–671.

Frenkel', M. Ya., Yaroshevsky, A. A., Ariskin, A. A., Barmina, G. S., Koptev-Dvornikov, E. V. & Kireev, B. S. (1988). *Dynamics of* in situ *Differentiation of Mafic Magmas*. Moscow: Nauka, 216 pp. (in Russian).

Frenkel', M. J., Yaroshevsky, A. A., Ariskin, A. A., Barmina, G. S., Koptev-Dvornikov, E. V. & Kireev, B. S. (1989). Convective–cumulative model simulating the formation process of stratified intrusions. In: Bonin, B., Didier, J., Le Fort, P., Propach, G., Puga, E. & Vistelius, A. B. (eds) *Magma–Crust Interactions and Evolution*. Athens: Theophrastus, pp. 3–88.

Froelich, A. J. & Gottfried, D. (1988). An overview of early Mesozoic intrusive rocks in the Culpeper basin, Virginia and Maryland. *Geological Society of America, Special Papers* **1776**, 151–164.

Fujii, T. (1974). Crystal settling in sills. *Lithos* **7**, 133–137.

Gibb, F. G. F. (1968). Flow differentiation in the xenolithic ultrabasic dykes of the Cuillins and the Strathaird Peninsula, Isle of Skye, Scotland. *Journal of Petrology* **9**, 411–443.

Gibb, F. G. F. (1972). A differentiated ultrabasic sheet on Sgurr Dearg, Isle of Skye. *Mineralogical Magazine* **38**, 811–818.

Gibb, F. G. F. & Henderson, C. M. B. (1978). The petrology of the Dippin sill, Isle of Arran. *Scottish Journal of Geology* **20**, 1–27.

Gibb, F. G. F. & Henderson, C. M. B. (1989). Discontinuities between picritic and crinanitic units in the Shiant Isles sill: evidence of multiple intrusion. *Geological Magazine* **126**, 127–137.

Gibb, F. G. F. & Henderson, C. M. B. (1992). Convection and crystal settling in sills. *Contributions to Mineralogy and Petrology* **109**, 538–545.

Gibb, F. G. F. & Henderson, C. M. B. (1996). The Shiant Isles Main Sill: structure and mineral fractionation trends. *Mineralogical Magazine* **60**, 67–97.

Gibson, S. A. & Jones, A. P. (1991). Igneous stratigraphy and internal structure of the Little Minch Sill Complex, Trotternish Peninsula, northern Skye, Scotland. *Geological Magazine* **128**, 51–66.

Gisselø, P. G. (2001). Sorgenfri Gletscher Sill Complex, East Greenland: solidification mechanisms of sheet-like bodies and the role of sill complexes in large igneous provinces. Ph.D. thesis, University of Aarhus.

Gorring, M. L. & Naslund, H. R. (1995). Geochemical reversals within the lower 100 m of the Palisades sill, New Jersey. *Contributions to Mineralogy and Petrology* **119**, 263–276.

Gray, N. H. & Crain, I. K. (1969). Crystal settling in sills: a model for suspension settling. *Canadian Journal of Earth Sciences* **6**, 1211–1216.

Grove, T. L. & Bence, A. E. (1977). Experimental study of pyroxene–liquid interaction in quartz-normative basalt 15597. *Proceedings of the 8th Lunar Science Conference. Geochimica et Cosmochimica Acta Supplement* 1549–1580.

Gunn, B. M. (1962). Differentiation in Ferrar Dolerites, Antarctica. *New Zealand Journal of Geology and Geophysics* **5**, 820–863.

Gunn, B. M. (1966). Modal and element variation in Antarctic tholeiites. *Geochimica et Cosmochimica Acta* **30**, 881–920.

Hamilton, W. (1965). Diabase sheets of the Taylor Glacier region, Victoria Land, Antarctica. *US Geological Survey, Professional Papers* **456-B**, 71.

Hanski, E. J. (1992). *Petrology of the Pechenga Ferropicrites and Cogenetic, Ni-bearing Gabbro–Wehrlite Intrusions at Pechenga, Kola Peninsula, Russia. Geological Survey of Finland Bulletin* **367**, 192 pp.

Henderson, C. M. B. & Gibb, F. G. F. (1987). The petrology of the Lugar sill, SW Scotland. *Transactions of the Royal Society of Edinburgh (Earth Sciences)* **77**, 325–347.

Heyn, J., Marsh, B. D. & Wheelock, M. M. (1995). Crystal size and cooling time in the Peneplain sill, Dry Valley Region, Antarctica. *Antarctic Journal of the United States* **30**, 50–51.

Hort, M., Marsh, B. D., Resmini, R. G. & Smith, M. K. (1999). Convection and crystallization in a liquid cooled from above: an experimental and theoretical study. *Journal of Petrology* **40**, 1271–1300.

Huppert, H. E. & Sparks, R. S. J. (1989). Chilled margins in igneous rocks. *Earth and Planetary Science Letters* **92**, 397–405.

Husch, J. M. (1990). Palisades sill: origin of the olivine zone by separate magmatic injection rather than gravity settling. *Geology* **18**, 699–702.

Irvine, T. N. (1970). Crystallization sequences in the Muskox intrusion and other layered intrusions. I. Olivine–pyroxene–plagioclase relations. *Geological Society of South Africa, Special Publication* **1**, 441–476.

Ivanov, M. K., Ivanova, T. K., Tarasov, A. V. & Shatkov, V. A. (1971). Petrology and ore mineralization peculiarities of differentiated intrusions of the Noril'sk ore junction (Noril'sk I, Noril'sk II and Chernaya Mountain deposits). In: Urvantstev, N. N. (ed.) *Petrology and Ore Mineralization of the Talnakh and Noril'sk Differentiated Intrusions. Trudy NIIGA* **167**, 197–305 (in Russian).

Jaupart, C. & Tait, S. (1995). Dynamic of differentiation in magma reservoirs. *Journal of Geophysical Research* **100**, 17617–17636.

Komar, P. D. (1972). Mechanical interactions of phenocrysts and flow differentiation of igneous dikes and sills. *Geological Society of America Bulletin* **83**, 973–988.

Kouchi, A., Tsuchiyama, A. & Sunagawa, I. (1986). Effect of stirring on crystallization kinetics of basalt: texture and element partitioning. *Contributions to Mineralogy and Petrology* **93**, 429–438.

Kretz, R., Hartree, R. & Garrett, D. (1985). Petrology of the Grenville swarm of gabbro dikes, Canadian Precambrian Shield. *Canadian Journal of Earth Sciences* **22**, 53–71.

Langmuir, C. H. (1989). Geochemical consequences of *in situ* crystallization. *Nature* **340**, 199–205.

Latypov, R. M. (2002). Phase equilibria constraints on relations of ore-bearing intrusions with flood basalts in the Noril'sk region, Russia. *Contributions to Mineralogy and Petrology* **143**, 438–449.

Latypov, R. M. (2003). The origin of marginal compositional reversals in basic–ultrabasic sills and layered intrusions by Soret fractionation. *Journal of Petrology* **44**, 1579–1618.

Latypov, R. M., Mitrofanov, F. F., Alapieti, T. T. & Halkoaho, T. A. A. (1999*a*). Petrology of the Lower Layered Horizon of the Western Pansky Tundra intrusion, Kola Peninsula. *Petrology* **7**, 509–538.

Latypov, R. M., Mitrofanov, F. P., Alapieti, T. T. & Kaukonen, R. J. (1999*b*). Petrology of Upper Layered Horizon (LLH) of West-Pansky intrusion, Kola Peninsula, Russia. *Russian Geology and Geophysics* **40**, 1434–1456.

Latypov, R. M., Dubrovskii, M. I. & Alapieti, T. T. (2001). Graphical analysis of the orthopyroxene–pigeonite–augite–plagioclase equilibrium at liquidus temperatures and low pressure. *American Mineralogist* **86**, 547–554.

Lebedev, A. P. (1957) About types of differentiation in traps of Siberian Platform. *Trudy Akademii Nauk SSSR Geologicheskaya Seriya* **2**, 55–74 (in Russian).

Lesher, C. E. & Walker, D. (1991). Thermal diffusion in petrology. In: Ganguly, J. (ed.) *Diffusion, Atomic Ordering, and Mass Transport: Selected Topics in Geochemistry. Advances in Physical Geochemistry 8*. New York: Springer, pp. 396–451.

Lewis, J. V. (1908). The Palisades diabase in New Jersey. *American Journal of Science* **176**, 155–162.

Likhachev, A. P. (1965). The role of the leucocratic gabbro in the formation of the ore-bearing differentiated intrusions of the Noril'sk region. Ph.D. thesis, University of Moscow (in Russian).

Likhachev, A. P. (1977). The conditions, which determined the formation of the trap magmas in the NW part of the Siberian platform. *Zapiski VMO* **6**, 594–605 (in Russian).

Likhachev, A. P. (1994). Ore-bearing intrusions of the Noril'sk region. *Proceedings of the Sudbury–Noril'sk Symposium. Ontario Geological Survey Special Publication* **5**, 185–201.

Lofgren, G. E. (1977). Dynamic crystallization experiments bearing on the origin of textures in impact-generated liquids. *Proceedings of the 8th Lunar Science Conference. Geochimica et Cosmochimica Acta Supplement* 2079–2095.

Lofgren, G. E. (1980). Experimental studies on the dynamic crystallization of silicate melts. In: Hargraves, R. B. (ed.) *Physics of Magmatic Processes*. Princeton, NJ: Princeton University Press, pp. 487–551.

Lofgren, G. E. (1983). Effect of heterogeneous nucleation on basaltic textures: a dynamic crystallization study. *Journal of Petrology* **24**, 229–255.

Lofgren, G. E., Donaldson, C. H., Williams, R. J., Mullins, O. & Usselman, T. M., Jr (1974). Experimentally reproduced textures and mineral chemistry of Apollo 15 quartz normative basalts. *Proceedings of the 5th Lunar Science Conference. Geochimica et Cosmochimica Acta Supplement* 549–567.

Lofgren, G. E., Donaldson, C. H. & Usselman, T. M. (1975). Geology, petrology, and crystallization of Apollo 15 quartz-normative basalts. *Proceedings of the 6th Lunar Science Conference. Geochimica et Cosmochimica Acta Supplement* 79–99.

Mangan, T. M. & Marsh, B. D. (1992). Solidification front fractionation in phenocryst-poor sheet-like magma bodies. *Journal of Geology* **100**, 605–620.

Mangan, T. M., Wright, T. L., Swanson, D. A. & Byerly, G. R. (1986). Regional correlation of Grande Ronder Basalt flows, Columbia River Basalt Group, Washington, Oregon and Idaho. *Geological Society of America Bulletin* **97**, 1300–1318.

Mangan, T. M., Marsh, B. D., Froelich, A. J. & Gottfried, D. (1993). Emplacement and differentiation of the York Haven diabase sheet, Pennsylvania. *Journal of Petrology* **34**, 1271–1302.

Marakushev, A. A., Fenogenov, A. N. & Emel'yanenko, P. F. (1982). Genesis of layered intrusions of the Noril'sk type. *Bulleten' Moskovskogo Universiteta, Geologicheskaya Seriya* **1**, 3–19 (in Russian).

Marsh, B. D. (1988). Crystal capture, sorting, and retention in convecting magma. *Geological Society of America Bulletin* **100**, 1720–1737.

Marsh, B. D. (1989). On convective style and vigor in sheet-like magma chambers. *Journal of Petrology* **30**, 479–530.

Marsh, B. D. (1990). Crystal capture, sorting, and retention in convective magma: Reply. *Geological Society of America Bulletin* **102**, 849–850.

Marsh, B. D. (1991). Reply to comments on 'On convective style and vigor in sheet-like magma chambers'. *Journal of Petrology* **32**, 855–860.

Marsh, B. D. (1996). Solidification fronts and magmatic evolution. *Mineralogical Magazine* **60**, 5–40.

Marsh, B. D. (1998). On the interpretation of crystal size distributions in magmatic systems. *Journal of Petrology* **39**, 553–599.

Marsh, B. D. & Wheelock, M. M. (1994). The vertical variation of composition in the Peneplain sill and Basement sills of the Dry Valleys: the Null Hypothesis. *Antarctic Journal of the United States* **29**, 25–26.

McBirney, A. R. & Noyes, R. M. (1979). Crystallization and layering of the Skaergaard intrusion. *Journal of Petrology* **20**, 487–554.

McDougall, I. (1962). Differentiation of the Tasmanian Dolerites: Red Hill dolerite–granophyre association. *Geological Society of America Bulletin* **73**, 279–316.

Morse, S. A. (1980). *Basalts and Phase Diagrams*. New York: Springer, 493 pp.

Naldrett, A. J. & Mason, G. D. (1968). Contrasting Archean ultramafic igneous bodies in Dundonald and Clergue Townships, Ontario. *Canadian Journal of Sciences* **5**, 111–143.

Naslund, H. R. (1989). Petrology of the Basistoppen sill, East Greenland: a calculated magma differentiation trend. *Journal of Petrology* **30**, 299–319.

Nekrasov, I. Ya. & Gorbachev, N. C. (1978). Physicochemical conditions of formation of the differentiated intrusions and copper–nickel ores of the Noril'sk type. *Ocherki Fiziko-Khimicheskoi Petrologii* **7**, 92–123 (in Russian).

Nielson, R. L. & De Long, S. E. (1992) A numerical approach to boundary layer fractionation: application to differentiation in natural magma systems. *Contributions to Mineralogy and Petrology* **110**, 355–369.

Richardson, S. H. (1979). Chemical variation induced by flow differentiation in an extensive Karroo dolerite sheet, southern Namibia. *Geochimica et Cosmochimica Acta* **43**, 1433–1441.

Rogover, G. B. (1959). *Noril'sk I Deposit*. Moscow: Gosgeoltechizdat, 168 pp. (in Russian).

Ryabov, V. V. (1992). *Olivines of the Siberian Traps as Indices of Petrogenesis and Ore Formation*. Novosibirsk: Nauka, 117 pp. (in Russian)

Shirley, D. N. (1987). Differentiation and compaction in the Palisades sill, New Jersey. *Journal of Petrology* **28**, 835–865.

Simkin, T. (1967). Flow differentiation in the picritic sills of north Skye. In: Wyllie P. J. (ed.) *Ultramafic and Related Rocks*. New York: Wiley, pp. 64–69.

Sinitsin, A. V. (1965). About distribution of microelements in differentiated intrusion of gabbrodolerite of Guby Ivanovskoy (Eastern Murmansk coast). *Trudy Akademii Nauk SSSR Geologicheskaya Seriya* **7**, 50–64 (in Russian).

Smirnov, M. F. (1966). *The Structure of Noril'sk Nickel-bearing Intrusions and Sulphide Ores*. Moscow: Nedra, 58 pp. (in Russian).

Smolkin, V. F. (1977). *Petrology of the Pilgujärvi Ore-bearing Intrusion*. Apatity: VINITI, N 2114-77, 216 pp. (in Russian).

Sparks, R. S. J., Huppert, H. E. & Turner, J. S. (1984). The fluid dynamics of evolving magma chambers. *Philosophical Transactions of the Royal Society of London, Series A* **310**, 511–534.

Steiner, J. C. (1992). A cumulus–transport–deposition model for the differentiation of the Palisades Sill. *Geological Society of America, Special Papers* **268**, 193–217.

Stone, W. E., Jensen, L. S. & Church, W. R. (1987). Petrography and geochemistry of an unusual Fe-rich basaltic komatiite from Boston Township, northeastern Ontario. *Canadian Journal of Earth Sciences* **24**, 2537–2550.

Stone, W. E., Crocket, J. H. & Fleet, M. E. (1995). Differentiation processes in an unusual iron-rich alumina-poor Archean ultramafic/mafic igneous body, Ontario. *Contributions to Mineralogy and Petrology* **119**, 287–300.

Tait, S. & Jaupart, C. (1992). Compositional convection in a reactive crystalline mush and melt differentiation. *Journal of Geophysical Research* **97**, 6735–6756.

Tait, S. & Jaupart, C. (1996). The producing of chemically stratified and adcumulate plutonic igneous rocks. *Mineralogical Magazine* **60**, 99–114.

Tait, S. R., Huppert, H. E. & Sparks, R. S. J. (1984). The role of compositional convection in the formation of adcumulate rocks. *Lithos* **17**, 139–146.

Tegner, C., Wilson, J. R. & Brooks, C. K. (1993). Intraplutonic quench zones in the Kap Edvard Holm Layered Gabbro Complex, East Greenland. *Journal of Petrology* **34**, 681–710.

Todd, S. G., Keith, D. W., Schissel, D. J., LeRoy, L. L., Mann, E. L. & Irvine, T. N. (1982). The J-M platinum–palladium reef of the Stillwater Complex, Montana: I. Stratigraphy and petrology. *Economic Geology* **77**, 1454–1480.

Turovtsev, D. M., Sluzhenikin, S. F. & Distler, V. V. (2000). Petrology of basic–ultrabasic layered massifs of the North Siberia and Southern Taimyr in connection with their PGE potentiality. *Petrography on the Verge of the XXI Century (Results and Perspectives). Proceedings of the Second All-Russia Petrographic Meeting*. Syktyvkar: Institute of Geology Komi, SC UD RAS, **4**, pp. 309–313.

Usselman, T. M., Lofgren, G. E., Donaldson, C. H. & Williams, R. J. (1975). Experimental modelling of the cooling history of Apollo 12 olivine basalts. *Proceedings of the 6th Lunar Science Conference*. *Geochimica et Cosmochimica Acta Supplement* 997–1020.

Vuollo, J. I. (1988). Petrology of the Koli sill: Kaunisniemi profile. *Report 14, Northern Karelia Ore Project*. Oulu: University of Oulu, 122 pp.

Wager, L. R. & Brown, G. M. (1968). *Layered Igneous Rocks*. Edinburgh: Oliver and Boyd, 588 pp.

Walker, D., Kirkpatrick, R. J., Longhi, J. & Hays, J. F. (1976). Crystallization history of lunar picritic basalt sample 12002: phase-equilibria and cooling-rate studies. *Geological Society of America Bulletin* **87**, 646–656.

Walker, F. (1940). The differentiation of the Palisades diabase, New Jersey. *Geological Society of America Bulletin* **51**, 1059–1106.

Walker, K. R. (1969). *The Palisades Sill, New Jersey: a Re-investigation. Geological Society of America, Special Papers* **111**, 178 pp.

Walker, K. R., Ware, N. G. & Lovering, J. F. (1973). Compositional variations in the pyroxenes of the differentiated Palisades sill, New Jersey. *Geological Society of America Bulletin* **84**, 89–110.

Woster, M. G., Huppert, H. E. & Sparks, R. S. J. (1990). Convection and crystallization in magma cooled from above. *Earth and Planetary Science Letters* **101**, 78–89.

Woster, M. G., Huppert, H. E. & Sparks, R. S. J. (1993). The crystallization in lava lakes. *Journal of Geophysical Research* **98**(B9), 15891–15901.

Wyllie, P. J. & Drever, H. I. (1963). The petrology of picritic rocks in minor intrusions—a picrite sill on the island of Soay (Hebrides). *Transactions of the Royal Society of Edinburgh* **65**, 155–177.

Yoder, H. S. (1965). Diopside–anorthite–water at five and ten kilobars and its bearing on explosive volcanism. *Carnegie Institution of Washington, Yearbook* **64**, 82–89.

Yoder, H. S. & Tilley, C. E. (1962). Origin of basalt magmas: an experimental study of natural and synthetic rock systems. *Journal of Petrology* **3**, 342–532.

Zen'ko, T. E. (1983). Mechanism of formation of the Noril'sk ore-bearing intrusions. *Trudy Akademii Nauk SSSR Geologicheskaya Seriya* **11,** 21–39 (in Russian).

Zolotuhin, V. V. & Vasil'ev, Yu. P. (1967). *Peculiarities of Mechanism of the Formation of Trap Ore-bearing Intrusions in NW Siberian Platform*. Moscow: Nauka, 231 pp. (in Russian).